The interaction between NARF and NLK observed in the yeast system was next examined in mammalian cells. T7-tagged NARF (T7-NARF) and FLAG-tagged full-length NLK (FLAG-NLK-WT) were co-expressed in 293 cells, and cell lysates were subjected to immunoprecipitation with anti-FLAG antibody. As shown in Fig. 1*B*, T7-NARF was co-immunoprecipitated with FLAG-NLK-WT and FLAG-NLK-ΔN (Fig. 1*B*, *lanes 5* and *7*), but not with FLAG-NLK-ΔC (Fig. 1*B*, *lane 6*). These results suggest that NARF specifically associates with the carboxyl-terminal region of NLK in mammalian cells.

To prove the existence of the endogenous NLK and NARF complex, extracts isolated from CaCO-2, SW480, and C2C12 cells were subjected to co-immunoprecipitation analysis using anti-NLK and NARF antibodies. Endogenous NARF was co-immunoprecipitated in these samples (Fig. 1*C* and data not shown). We conclude that NLK and NARF can form a complex in cells.

NARF Exhibits Auto-ubiquitylating Activity Associated with E2-25K—Recent data indicate that numerous RING finger proteins can function as E3 ubiquitin-ligases. To determine whether NARF may interact with a partner protein(s) in the ubiquitylation system, we attempted to identify protein(s) that physiologically interact with NARF in mammalian cells. FLAG-tagged NARF (FLAG-NARF) was expressed in 293 cells, and NARF and associated proteins were recovered from cell extracts by immunoprecipitation with anti-FLAG antibody. The precipitated proteins were eluted with a FLAG peptide and digested with Lys-C endopeptidase. The cleaved fragments were directly analyzed and sequenced by nanoflow LC-MS/MS. A data base search of the peptide sequences obtained identified one of the E2 ubiquitin-conjugating enzymes, E2-25K, as a NARF-interacting protein (Table 1). The interaction between NARF and E2-25K was confirmed with transiently expressed HA-tagged E2-25K (HA-E2-25K) and FLAG-NARF in 293 cells (Fig. 2*A*, *lane 3*). To define whether NARF mediates ubiquitylation as an E3 ubiquitin-ligase, we performed an *in vitro* auto-ubiquitylation assay for NARF using E2-25K as an E2 conjugating enzyme. We generated a GST fusion with wild-type NARF (GST-NARF-WT), and incubated this with purified E1 ubiquitin-activating enzyme, E2-25K, and ubiquitin. Western blotting analysis showed that NARF was poly-ubiquitylated, as indicated by the appearance of a broad ladder detected with either anti-ubiquitin (Ub) antibody (Fig. 2*B*, *lanes 5–8*) or anti-GST antibody (Fig. 2*B*, *lanes 21–24*). GST-NARF-WT ubiquitylation levels increased in a time-dependent manner (Fig. 2*B*, *lanes 5–8* and *21–24*), and required the presence of E2-25K (Fig. 2*B*, *lanes 1–4* and

TABLE 1
Identification of human E2-25K by LC-MSMS
Sequence coverage was 30%.

Sequence determined	Peptide	Charge	Residues
	m/z		
ANIAVQRIK	527.8	2	2–10
IWHPNISSVTGAICLDILK	713.1	3	28–46
IPETYPFNPPK	651.8	2	62–72
IENLCAMGFDRNAVIVALSSK	770.1	3	115–135

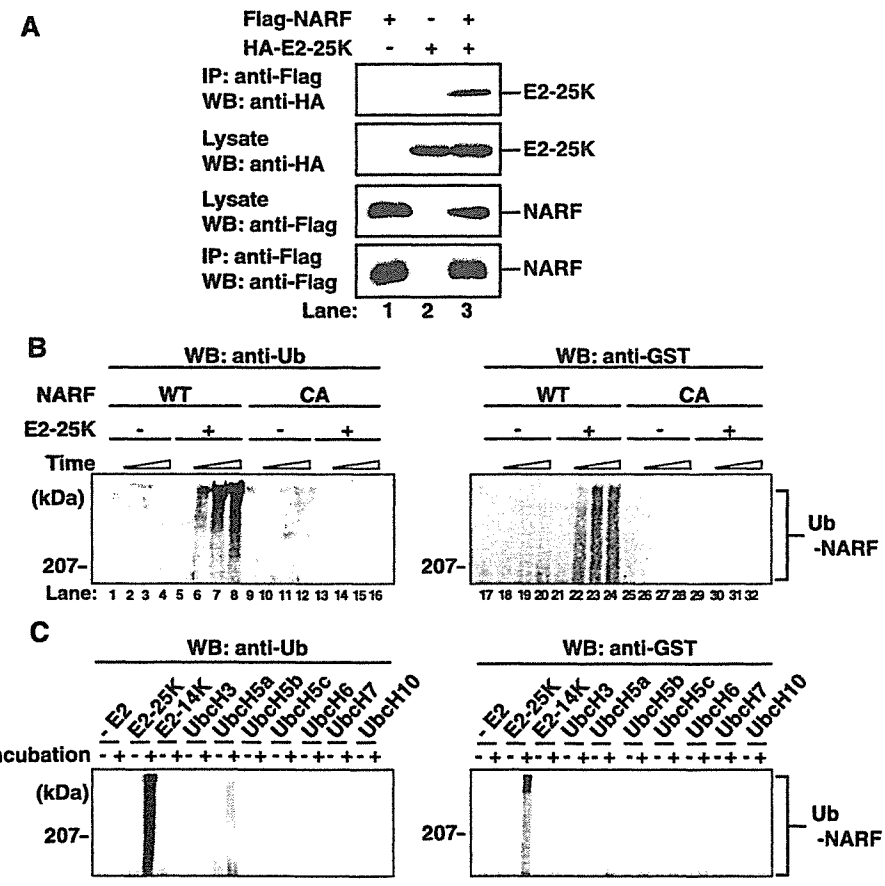

FIGURE 2. **NARF exhibits E3 ubiquitin-ligase activity in cooperation with the ubiquitin conjugating enzyme, E2-25K.** *A*, E2 ubiquitin-conjugating enzyme E2-25K was identified as a NARF-associating protein by LC-MS/MS analysis. Interaction between NARF and E2-25K was confirmed in 293 cells transiently expressing FLAG-NARF and HA-E2-25K. Whole cell lysates were subjected to immunoprecipitation (*IP*) with anti-FLAG antibody, followed by Western blotting analysis (*WB*) with anti-HA antibody to detect HA-E2-25K co-immunoprecipitated with FLAG-NARF (*top panel*). *B*, *in vitro* ubiquitylation assay was performed with bacterially expressed GST-NARF wild-type (*WT*) or RING finger domain mutant (*CA*). GST-NARF was incubated with purified rabbit E1, bovine ubiquitin, and human E2-25K at 30 °C for 0, 30, 60, or 90 min. The reaction mixtures were resolved by SDS-PAGE, and Western blotting analysis with both anti-Ub antibody (*left panel*) and anti-GST antibody (*right panel*) detected the state of GST-NARF-WT poly-ubiquitylation. *C*, *in vitro* ubiquitylation assay of GST-NARF was performed with a panel of E2-conjugating enzymes including E2-25K, E2-14K, UbcH3, UbcH5a, UbcH5b, UbcH5c, UbcH6, UbcH7, and UbcH10. The reaction mixtures were incubated for 0 (−) or 120 min (+). Poly-ubiquitylated GST-NARF was detected by Western blotting analysis with anti-Ub antibody (*left panel*) and anti-GST antibody (*right panel*).

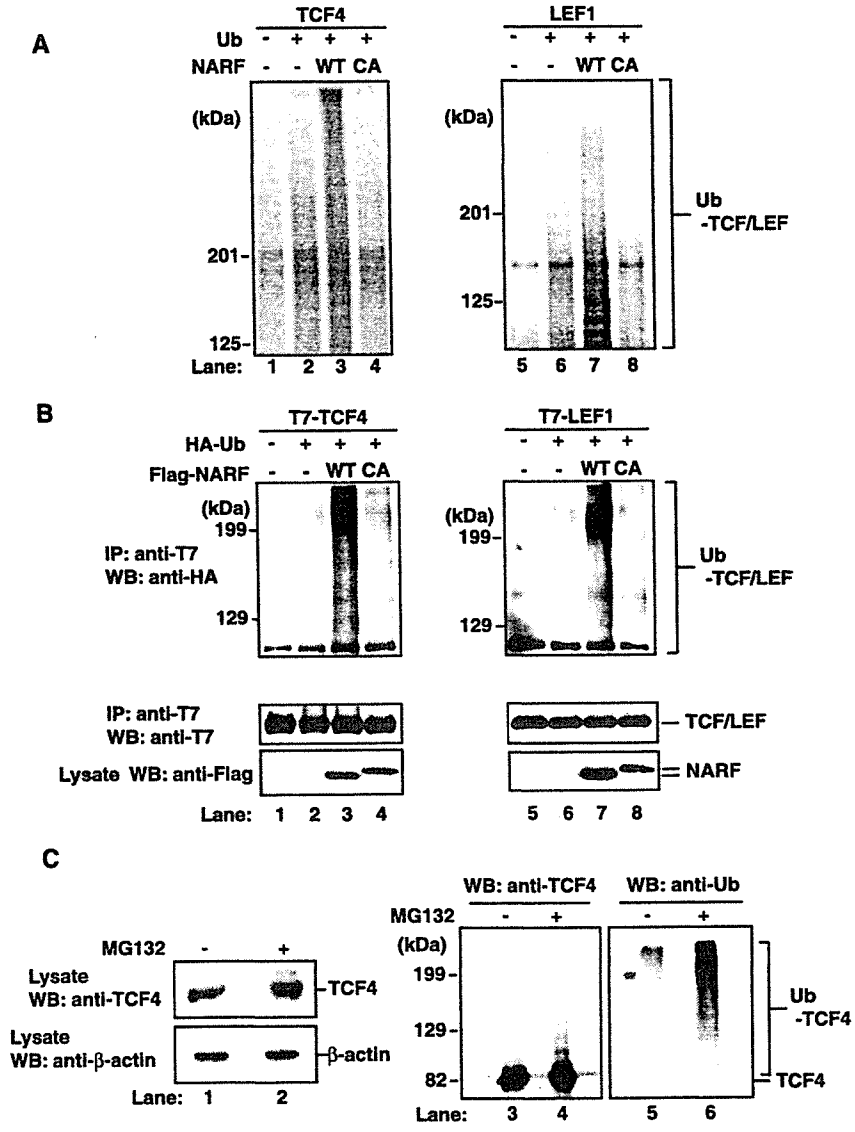

FIGURE 3. **NARF ubiquitylates the transcription factors TCF/LEF.** *A*, ^{35}S-labeled recombinant TCF4 or LEF1 was prepared by an *in vitro* transcription/translation system, and used as a substrate for an *in vitro* ubiquitylation assay with GST-NARF wild-type (GST-NARF-WT) or RING finger domain mutant (GST-NARF-CA). Poly-ubiquitylated ^{35}S-labeled TCF4 and LEF1 were detected by autoradiography (*lanes 3* and *7*). *B*, T7-TCF4 or T7-LEF1 were co-expressed with HA-ubiquitin (*HA-Ub*) and FLAG-NARF in 293 cells. T7-TCF4 or LEF1 were immunoprecipitated by anti-T7 antibody from whole cell lysates, and the poly-ubiquitylated states of each were detected by Western blot (*WB*) analysis with anti-HA antibody (*top panels, lanes 3* and *7*). Western blot analysis with anti-T7 antibody (*middle panels*) or anti-FLAG antibody (*bottom panels*) using whole cell lysates confirmed that there were equivalent levels of expressed recombinant proteins in each experiment. *C*, 293 cells were incubated with 10 μM of the proteasome inhibitor MG132 for 4 h, and whole cell lysates were analyzed by Western blot analysis with anti-TCF4 antibody (*upper left panel*) or anti-β-actin antibody (*lower left panel*). Endogenous TCF4 was immunoprecipitated (*IP*) with anti-TCF4 antibody, and analyzed with both anti-TCF4 antibody and anti-Ub antibody (*two right panels*).

17–20). It is noteworthy that no GST-NARF-WT ubiquitylation was observed when the two conserved cysteine residues at 17 and 53 within the RING finger domain were replaced with alanine (GST-NARF-CA, Fig. 2*B*, *lanes 13–16* and *29–32*). To clarify whether E2-25K is an authentic E2-conjugating enzyme for NARF in the ubiquitylation process, we assayed GST-NARF-WT auto-ubiquitylation using a panel of E2-conjugating enzymes (E2-25K, E2-14K, UbcH3, UbcH5a, UbcH5b, UbcH5c, UbcH6, UbcH7, and UbcH10). Fig. 2*C* showed that auto-ubiquitylation of GST-NARF-WT occurred most robustly in the presence of E2-25K among the examined E2 enzymes, although other E2 enzymes also mediated weak ubiquitylation. These data show that the auto-ubiquitylating activity of NARF is coordinated with E2-25K, and that the RING finger domain of NARF is indispensable for this reaction.

NARF Ubiquitylates the Transcription Factor TCF/LEF—To clarify the biological role of NARF, we initially searched for target proteins that are ubiquitylated by NARF. Although NARF was isolated as an NLK-associating protein, NARF did not ubiquitylate NLK in an *in vitro* ubiquitylation assay (data not shown). Therefore, we examined further the possibility that NARF may ubiquitylate NLK-associated transcription factors or other Wnt signaling components. We used rabbit reticulocytes to prepare ^{35}S-labeled recombinant proteins for each candidate substrate of NARF-directed ubiquitylation, and incubate each, together with GST-NARF-WT or GST-NARF-CA, in an *in vitro* ubiquitylation assay (data not shown). From this series of assays, we found that NARF-WT could ubiquitylate the transcription factor TCF/LEF, as indicated by the appearance of a ladder of bands (Fig. 3*A*, *lanes 3* and *7*). TCF/LEF ubiquitylation was not observed with NARF-CA, which does not have ubiquitin ligase activity as shown in Fig. 3*B* (Fig. 3*A*, *lanes 4* and *8*). These results indicate that NARF ubiquitylates TCF/LEF and this activity requires its RING finger domain structure.

To ascertain whether TCF/LEF is actually ubiquitylated in cells, T7-tagged TCF4 (T7-TCF4) or LEF1 (T7-LEF1) were co-expressed together with HA-tagged ubiquitin (HA-Ub) and FLAG-tagged NARF (FLAG-NARF-WT) in 293 cells, and cell lysates were immunoprecipitated with anti-T7 antibody. Poly-ubiquitylation of TCF4 or LEF1 was indicated by the appearance of a ladder in Western blots with anti-HA antibody (Fig. 3*B*, *lanes 3* and *7*). When the critical cysteine residues at 17 and 53 within the RING finger domain of NARF were mutated (FLAG-NARF-CA), ubiquitylation of T7-TCF/LEF by FLAG-NARF was abolished to basal levels (Fig. 3*B*, *lanes 4* and *8*). We also examined the association between endogenous TCF4, NLK, and

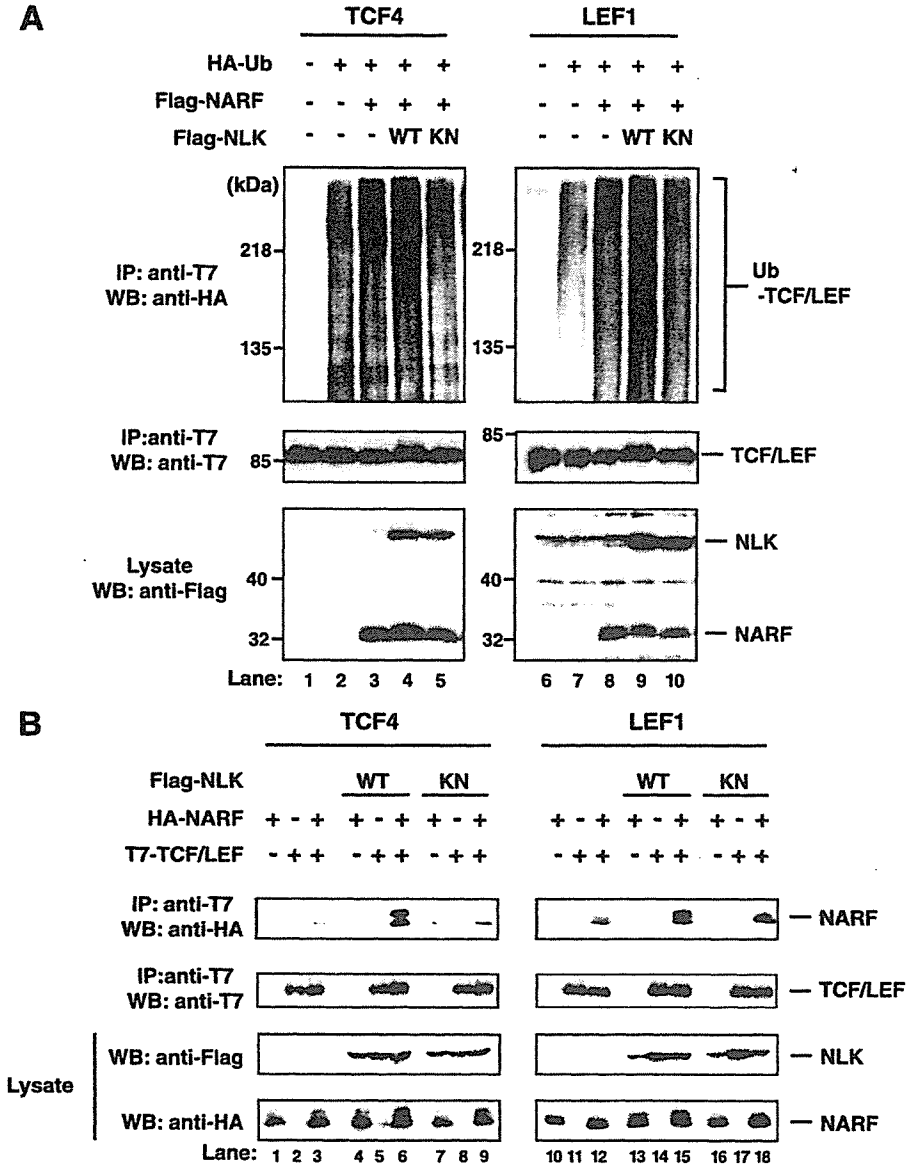

FIGURE 4. **NLK augments the ubiquitylation activity of NARF against TCF/LEF.** *A*, T7- TCF4/LEF1, FLAG-NARF, HA-ubiquitin (*Ub*), and FLAG-NLK wild-type (*WT*) or kinase-negative mutant (*KN*) were co-expressed in 293 cells. T7-TCF4 or T7-LEF1 were immunoprecipitated (*IP*) by an anti-T7 antibody from whole cell lysates and poly-ubiquitylated T7-TCF4 or T7-LEF1 were detected by Western blotting analysis (*WB*) with anti-HA antibody (*top panels*). Western blotting analysis with anti-T7 antibody (*middle panels*) or anti-FLAG antibody (*bottom panels*) using whole cell lysates confirmed that there were equivalent levels of expressed recombinant proteins in each experiment. *B*, HA-NARF and T7-TCF4 or T7-LEF1 were co-expressed with FLAG-NLK wild type (*WT*) or kinase-negative mutant (*KN*) in 293 cells. T7-TCF4 or T7-LEF1 were immunoprecipitated with anti-T7 antibody from whole cell lysates, and the association of HA-NARF with T7-TCF4 or T7-LEF1 was detected by anti-HA antibody (*top panels*). Western blotting analysis with anti-FLAG antibody (*second panels from top*), anti-HA antibody (*second panels from bottom*), or anti-T7 antibody (*bottom panels*) using whole cell lysates confirmed that there were equivalent levels of expressed recombinant proteins in each experiment.

NARF in 293 cells, and detected an interaction between endogenous NLK and TCF4, but not between NARF and TCF4 (data not shown). This result may raise the possibility that TCF4 is rapidly degraded after ubiquitylation by NARF. These data established that TCF/LEF is a candidate target for the ubiquitylation activity of NARF *in vivo*.

To verify the ubiquitylation of TCF/LEF *in vivo*, we attempted to detect ubiquitylation of the endogenous TCF4. When 293 cells were treated with the proteasome inhibitor MG132, endogenous TCF4 levels were markedly increased (Fig. 3*C*, *lane 2*) and an accumulation of poly-ubiquitylated TCF4 was detected with both anti-Ub antibody (Fig. 3*C*, *lane 6*) and anti-TCF4 antibody (Fig. 3*C*, *lane 4*). These results indicate that the ubiquitylation of TCF/LEF can occur under physiological conditions and also suggests that TCF/LEF protein stability is regulated via the ubiquitin-proteasome system.

NLK Augments the Ubiquitylation Activity of NARF against TCF/LEF—To examine the possibility that NLK regulates NARF function in the ubiquitylation of TCF/LEF *in vivo*, either T7-TCF4 or T7-LEF1 were co-expressed with HA-Ub and FLAG-NARF with or without FLAG-NLK in 293 cells. Poly-ubiquitylated T7-TCF4 or T7-LEF1 was immunoprecipitated by anti-T7 antibody and detected as a ladder of bands reacting with anti-HA antibody (Fig. 4*A*, *lanes 3* and *8*). When FLAG-tagged wild-type NLK (FLAG-NLK-WT) was co-expressed, ubiquitylation of T7-TCF4 or T7-LEF1 was significantly augmented (Fig. 4*A*, *lane 3 versus 4* and *lane 8 versus 9*), whereas no enhancement of ubiquitylation was observed when the kinase-inactive mutant FLAG-NLK (FLAG-NLK-KN) was co-expressed (Fig. 4*A*, *lane 3 versus 5* and *lane 8 versus 10*). To assess the cooperation of NLK in the interaction between NARF and TCF/LEF, HA-tagged NARF (HA-NARF) and T7-TCF4 or T7-LEF1 were co-expressed in 293 cells with or without FLAG-NLK. When T7-TCF4 or T7-LEF1 were immunoprecipitated from whole cell lysates with anti-T7 antibody, a weak association of HA-NARF was detected by anti-HA antibody in the absence of NLK co-expression (Fig. 4*B*, *lanes 3* and *12*). When FLAG-NLK wild-type (FLAG-NLK-WT) was co-expressed with HA-NARF and T7-TCF/LEF, the association between HA-NARF and T7-TCF4/LEF1 was apparently enhanced (Fig. 4*B*, *lanes 6* and *15*). However, no such enhancement was seen when kinase-inactive mutant NLK (FLAG-NLK-KN) was co-expressed (Fig. 4*B*, *lanes 9* and *18*). These data clearly indicate that NLK facilitates

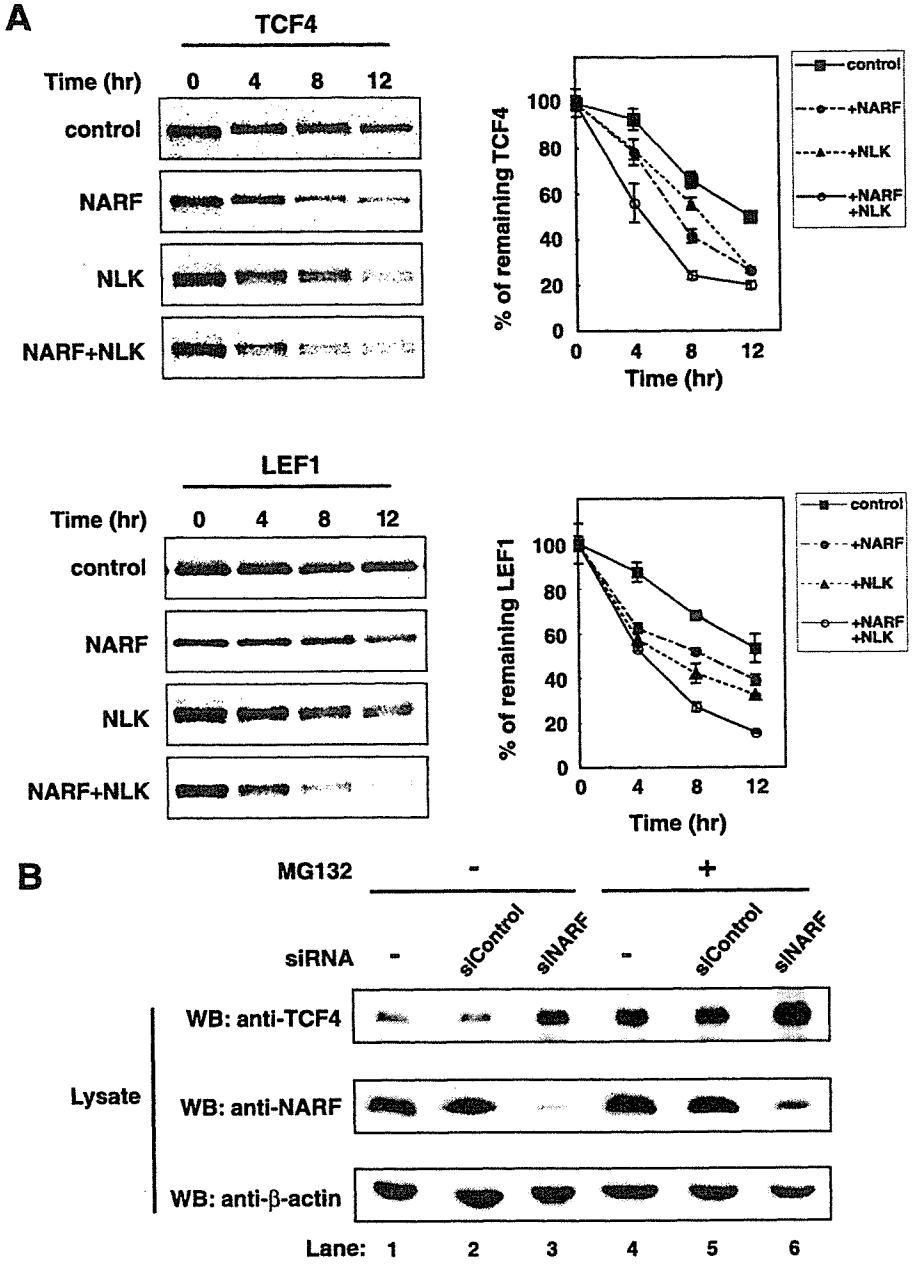

FIGURE 5. **NLK and NARF coordinate the degradation of TCF/LEF.** *A*, T7-TCF4 or T7-LEF1 was expressed with NARF and/or NLK in 293 cells. T7-TCF4 or T7-LEF1 were metabolically labeled with [^{35}S]methionine and cysteine, and chased for the indicated time periods. Cells were lysed in RIPA buffer, and [^{35}S]T7-TCF4 or [^{35}S]T7-LEF1 were immunoprecipitated with anti-T7 antibody. [^{35}S]T7-TCF4 or [^{35}S]T7-LEF1 were detected by autoradiography (*left panels*) and quantified from the intensity of the visualized bands (*right panels*). The half-life of TCF4 was calculated from a linear plot of the rate of [^{35}S]TCF4 decay in cells. *B*, the expression of endogenous NARF was suppressed by siRNA. 293 cells were transfected with siRNAs and treated with 10 μM MG132 or Me_2SO for 4 h. Control siRNA is targeted for luciferase. Expression of endogenous TCF4 and NARF were examined by Western blotting (*WB*) analysis with anti-TCF4 antibody (*top panel*) and anti-NARF peptide antibody (*middle panel*), respectively. β-Actin was used as a loading control (*bottom panel*).

NARF-directed ubiquitylation of TCF/LEF by enhancing the association between NARF and TCF/LEF, and that this enhancement depends on NLK kinase activity.

NLK and NARF Coordinate the Degradation of TCF/LEF—The preceding data demonstrated that TCF/LEF protein levels are regulated via the ubiquitin-proteasome pathway (Fig. 3*C*). To evaluate the effect of NARF and NLK on the protein stability of TCF/LEF, we performed pulse-chase experiments using TCF/LEF metabolically labeled with [^{35}S]methionine/cysteine in 293 cells. During the chase period, the level of ^{35}S-labeled TCF4 and LEF1 declined gradually and their half-lives were estimated to be 12.5 and 12.9 h, respectively (Fig. 5*A*, *control panels*). Interestingly, co-expression of NARF shortened the half-lives of TCF4 and LEF1 to 7.8 and 7.2 h (Fig. 5*A*, *NARF panels*), and co-expression of NLK shortened them to 8.6 and 5.7 h, respectively (Fig. 5*A*, *NLK panels*). Furthermore, it is intriguing that co-expression of both NARF and NLK dramatically reduced the protein stability of TCF4 and LEF1 to half-lives of 4.5 and 4.4 h, respectively. The doublet bands observed for TCF/LEF proteins when NLK was expressed might be due to NLK-induced phosphorylation, as described previously (4). These results are consistent with the data from ubiquitylation analysis, suggesting that NARF and NLK contribute to the regulation of TCF/LEF protein levels via the ubiquitin-mediated degradation pathway.

The physiological involvement of NARF in modulating TCF/LEF protein stability via ubiquitylation and the proteasome degradation was confirmed using siRNA. Introduction of siRNA targeting the human NARF mRNA into 293 cells effectively diminished the amount of endogenous NARF detected by anti-NARF antibody, and caused a significant accumulation of endogenous TCF4 in 293 cells (Fig. 5*B*, *lanes 1* and *2 versus 3*; and *lanes 4* and *5 versus 6*). Proteasome inhibitor treatment further enhanced the stability of endogenous TCF4 (Fig. 5*B*, *lane 1 versus 4*; *lane 2 versus 5*; and *lane 3 versus 6*), indicating that NARF physiologically regulates the fate of TCF4 via proteasome-mediated pathways in 293 cells. Interestingly, the levels of NARF protein also increased when cells were treated with MG132. As we had found that NARF itself was ubiquitylated in an *in vitro* ubiquitylation assay (see Fig. 2, *B* and *C*), we speculate that NARF might also be degraded through the proteasome system.

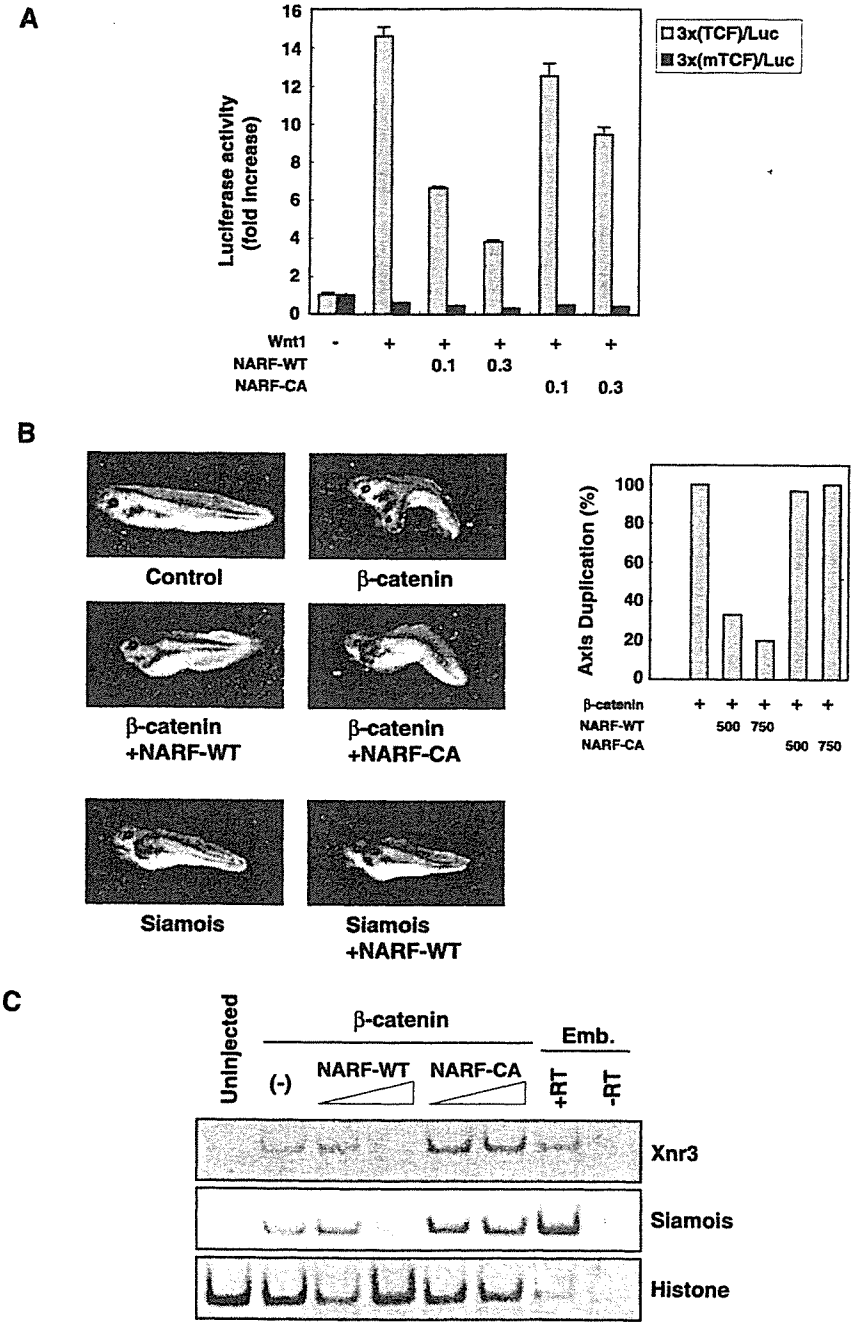

FIGURE 6. **NARF negatively regulates the Wnt signaling pathway.** *A*, 293 cells were transiently transfected with the expression vectors for Wnt-1, a luciferase reporter linked to the Wnt-responsive TCF-binding sites (*3x(TCF)/Luc*) or the mutated sites (*3x(mTCF)/Luc*), and either NARF wild-type (*NARF-WT*) or RING finger domain mutant (*NARF-CA*). Cells were harvested after 24 h post-transfection and assayed for luciferase activity. The transfection efficiency was normalized with the activity of co-transfected *Renilla* luciferase vector controlled by the EF-1α promoter. Values are expressed as the -fold increase in luciferase activity relative to the level of activity with reporter plasmid alone. *B*, synthetic mRNAs encoding *β-catenin* (100 pg) or *Siamois* (0.5 pg) were microinjected with *NARF-WT* mRNA (500 and 700 pg) or RING finger domain mutant mRNA (500 and 750 pg) into the ventral equatorial region of the 4-cell stage *Xenopus* embryos to induce secondary axis formation as indicated. The representative embryos are shown (*left panels*). The ectopic axis formations were counted at the tadpole stage and expressed as the ratio of axis-formed embryos to total examined numbers (n = 30, axis duplication %, *right panel*). *C*, RT-PCR analysis in animal caps. Synthetic mRNA encoding *β-catenin* (100 pg) was microinjected with *NARF-WT* mRNA (50 and 300 pg) or RING finger domain mutant mRNA (50 and 300 pg) into the animal pole of two blastomeres at the 2-cell stage *Xenopus* embryos. Animal cap explants were removed at the blastula stage. Total RNAs were prepared and analyzed by RT-PCR for the expression of Wnt target genes, *Xnr3* and *Siamois*. Histone was used as a loading control. *Emb* indicates whole embryo control with (*+RT*) or without (*−RT*) at the RT step.

NARF Negatively Regulates the Wnt Signaling Pathway—To investigate the effect of NARF on Wnt-induced, TCF/LEF-dependent transcriptional activity, a luciferase reporter plasmid containing Wnt-responsive TCF-binding sites, 3x(TCF)/Luc (38), was transfected into 293 cells, and the transcriptional activity of TCF/LEF was measured as shown in Fig. 6*A*. When an expression vector encoding wild-type NARF (*NARF-WT*) was co-transfected together with the reporter plasmid, Wnt-induced TCF/LEF-dependent transcriptional activity was suppressed in a dose-dependent manner down to 75% of the control. In contrast, expression of RING finger domain mutant NARF (*NARF-CA*) exhibited little effect on the TCF/LEF transcriptional activity. To further address the possibility that NARF suppresses the Wnt-β-catenin-mediated signaling pathway, NARF mRNA was co-injected into *X. laevis* embryos. Expression of the injected mRNAs in embryos was confirmed by Western blotting (data not shown). Normally, the secondary axis in *X. laevis* embryos is induced by ectopic expression of β-catenin. However, injection of wild-type NARF (*NARF-WT*) mRNA into the embryos significantly inhibited secondary axis formation and the target gene expression (*Xnr3* and *Siamois*) induced by β-catenin in a dose-dependent manner. In contrast, injection of the RING finger domain mutant NARF (*NARF-CA*) mRNA had no inhibitory effect on axis formation and gene expression (Fig. 6, *B* and *C*). Furthermore, injection of *NARF* or *NLK* mRNA into the 4-cell stage embryos did not produce any discernible phenotypic change in the embryos (data not shown). Moreover, injection of *NARF-WT* mRNA did not inhibit axis formation induced by Siamois (Fig. 6*B*). These results indicate that NARF specifically inhibits secondary axis formation and gene expression induced by β-catenin, and does

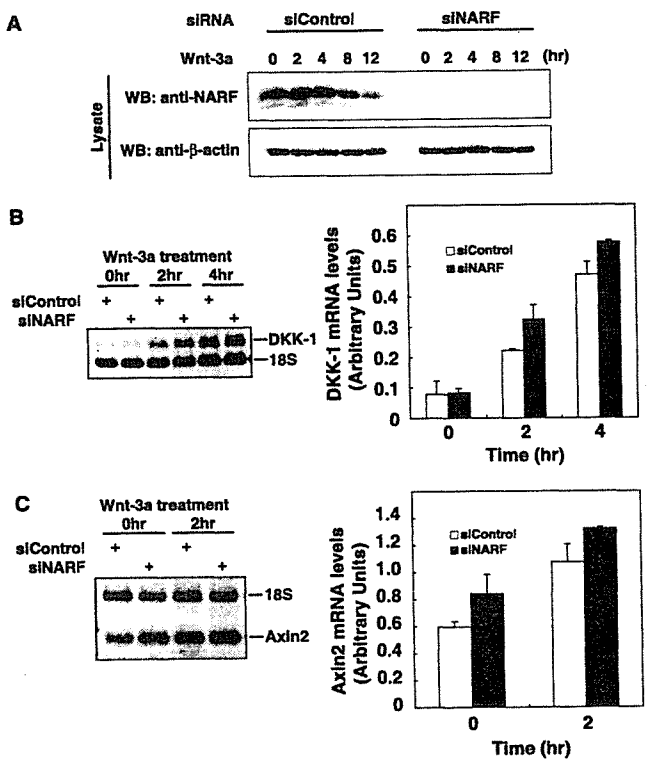

FIGURE 7. **Knockdown of the endogenous NARF enhances Wnt-3a-dependent *DKK-1* and *Axin2* gene expression.** *A*, HeLaS3, transiently transfected with control (*siControl*) or specific human NARF siRNA (*siNARF*), were treated with Wnt-3A conditioned medium for the indicated periods, and total cell lysates were subjected to SDS-PAGE and Western blotting (*WB*) analysis with anti-NARF antibody (*upper panel*). The loading control was carried out with an anti-β-actin antibody (*lower panel*). *B* and *C*, the effect of *siNARF* on Wnt-3A-induced *DKK-1* and *Axin2* mRNA expression. siRNA-treated HeLaS3 cells were incubated with Wnt-3A CM for the indicated time periods. Semi-quantitative multiplex RT-PCR was performed for 30 cycle amplifications with *DKK-1* primers or 35 cycle amplifications with *Axin2* primers, and Quantum RNA 18 S internal standards II. Representative SYBR Green I-stained PCR products are shown (*left panel*). *DKK-1* and *Axin2* expression were normalized to expression of the 18 S ribosomal RNA and presented as the ratio of fluorescence intensity of the *DKK-1* or *Axin2 versus* 18 S bands (*right panel*). Data are shown as the mean ± S.D. of the three separate experiments.

not act at some downstream signaling step, suggesting that NARF can negatively regulate Wnt-β-catenin signaling *in vivo*.

Knockdown of the Endogenous NARF Enhances Wnt-3a-dependent Genes Expression—To evaluate the physiological relevance of NARF to the canonical Wnt/β-catenin signaling pathway, we used siRNA to suppress expression of the endogenous NARF protein in HeLaS3 cells. We examined the effect of NARF siRNA on the expression of *Dickkopf-1* (*DKK-1*) and *Axin2*, target genes of Wnt/β-catenin signaling (39, 40). As shown in Fig. 7, *B* and *C*, Wnt-3a treatment induced the expression of the *DKK-1* and *Axin2* genes. When endogenous NARF expression was suppressed with NARF siRNA (siNARF) (Fig. 7*A*), Wnt-dependent expression of *DKK-1* and *Axin2* mRNAs were further enhanced as compared with the control (siControl) at all time points examined (Fig. 7, *B* and *C*). The data presented here are consistent with our notion that NARF is physiologically required for suppression of the Wnt/β-catenin-mediated signaling pathway.

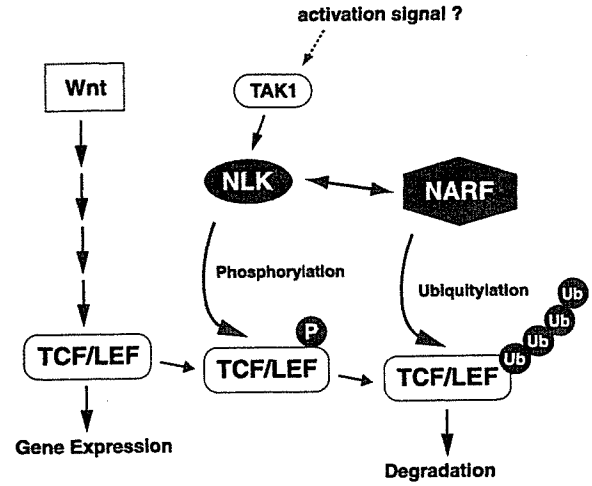

FIGURE 8. **A proposal model for the roles of NARF in the suppression of the Wnt-β-catenin signaling pathways.**

DISCUSSION

In the present study, we identified NARF as a NLK-binding protein and characterized its functions. Our results suggest that NARF is a RING finger-type E3 ubiquitin-ligase and is involved in the ubiquitylation of TCF/LEF. Furthermore, we demonstrate that NARF and E2-25K are indispensable for ubiquitylation and degradation of TCF/LEF. These activities require NLK-induced phosphorylation of TCF/LEF, as *in vitro* kinase assays demonstrated that NLK could phosphorylate TCF/LEF but not NARF (data not shown). These findings provide the first evidence that NARF functions in the specific ubiquitylation and degradation of TCF/LEF *in vivo*, and demonstrate the significance of NARF in Wnt signaling. Based on these data, we propose a model for the function of NARF in the ubiquitylation and degradation of TCF/LEF (Fig. 8). In cells at a steady state, NARF complexes with NLK. Activation of NLK induced by unknown ligands leads to the phosphorylation of TCF/LEF. NARF then acts on TCF/LEF as an E3 ubiquitin-ligase and, together with E1 and E2 ubiquitylation enzymes, catalyze the ubiquitylation of TCF/LEF. Finally, ubiquitylated TCF/LEF is degraded by the 26 S proteasome. Thus, we suggest that NARF is a key component that regulates the degradation of TCF/LEF and acts as a negative regulator of Wnt signaling.

We analyzed NARF-binding proteins using an LC-MS/MS system and identified E2-25K, an E2 ubiquitin-conjugating enzyme for ubiquitylation. This suggests that NARF is an E3 ubiquitin-ligase. We have previously shown that NLK, and TCF/LEF phosphorylation, negatively regulate Wnt signaling. These facts raise the possibility that TCF/LEF or other molecules involved in Wnt signaling may be targets of NARF E3 ubiquitin-ligase activity. We observed that TCF/LEF was ubiquitylated by NARF *in vitro* and *in vivo*. We also demonstrated that suppression of NARF expression by siRNA results in increased levels of expression of the Wnt-induced genes, DKK-1 and Axin2 (Fig. 7). This indicates that NARF plays a critical role in the endogenous regulation of Wnt signaling. Several reports have indicated that the sumoylation and acetylation of TCF/LEF regulates its subcellular localization and transcrip-

tional activity (41–43). Our results provide new evidence that ubiquitylation of TCF/LEF also plays a role in the regulation of cellular signaling. Although the biological significance of ubiquitylation of TCF/LEF is unclear at present, it is certain that NARF is involved in the degradation of TCF/LEF through the action of a yet to be identified ligand(s) that negatively regulates the Wnt signaling pathway. Further studies will be needed to identify the precise ligand that induces the activity of the NARF E3 ubiquitin-ligase involved in TCF/LEF ubiquitylation.

Our studies demonstrate that among the members of the Ubc family of E2 ubiquitin-conjugating enzymes, E2-25K can specifically support the ubiquitylation of TCF/LEF. Previous biochemical analyses have demonstrated that E2-25K is a unique E2 protein in the ubiquitin/proteasome system that is involved in the synthesis of poly-ubiquitin chains *in vitro* from mono- or poly-ubiquitin, E1, and ATP (44–46). Previous studies also indicated biological roles for E2-25K in neurodegenerative diseases, as a regulator of huntingtin in Huntingtin disease (47) and amyloid-β peptide neurotoxicity in Alzheimer disease (48). TCF/LEF is the first protein to be directly and specifically shown to be a substrate for E2-25K-dependent ubiquitylation by NARF, although it has not been definitively proven whether NARF, an E3 ubiquitin-ligase, is involved in any neurodegenerative disease at present.

The function of TCF/LEF in embryonic development has been intensively studied. We have shown previously that NLK plays an essential role in axis formation, mesoderm induction, and neural development in *Xenopus* embryos (4, 6, 11). Moreover, *Xenopus* NARF mRNA was expressed maternally and throughout early development (data not shown). Expression of NARF was observed to inhibit the secondary axis formation induced by ectopic expression of β-catenin in *Xenopus* embryos. These observations led us to hypothesize that NARF, a post-translational regulator of TCF/LEF stability, may also participate in the control of embryonic development. Further elucidation of the function of NARF may lead to the identification of novel mechanisms by which ubiquitylation induced by unknown ligands negatively regulates Wnt signaling. However, it remains to be shown how the specific ubiquitylation of TCF/LEF contributes to the diverse early developmental processes regulated by NARF in *Xenopus* embryos. Additional experiments will be required to assess the role of NARF in *Xenopus* development.

Acknowledgments—We thank K. Matsumoto and K. Shirakabe for excellent advice, M. Lamphier for critical reading of the manuscript, and S. Tobiume and K. Nakamura for technical assistance.

REFERENCES

1. Logan, C. Y., and Nusse, R. (2004) *Annu. Rev. Cell Dev. Biol.* **20,** 781–810
2. Cadigan, K. M., and Nusse, R. (1997) *Genes Dev.* **11,** 3286–3305
3. Brott, B. K., Pinsky, B. A., and Erikson, R. L. (1998) *Proc. Natl. Acad. Sci. U. S. A.* **95,** 963–968
4. Ishitani, T., Ninomiya-Tsuji, J., Nagai, S., Nishita, M., Meneghini, M., Barker, N., Waterman, M., Bowerman, B., Clevers, H., Shibuya, H., and Matsumoto, K. (1999) *Nature* **399,** 798–802
5. Meneghini, M. D., Ishitani, T., Carter, J. C., Hisamoto, N., Ninomiya-Tsuji, J., Thorpe, C. J., Hamill, D. R., Matumoto, K., and Bowerman, B. (1999) *Nature* **399,** 793–797
6. Ohkawara, B., Shirakabe, K., Hyodo-Miura, J., Matsuo, R., Ueno, N., Matsumoto, K., and Shibuya, H. (2004) *Genes Dev.* **18,** 381–386
7. Shibuya, H., Yamaguchi, K., Shirakabe, K., Tonegawa, A., Gotoh, Y., Ueno, N., Irie, K., Nishida, E., and Matsumoto, K. (1996) *Science* **272,** 1179–1182
8. Yamaguchi, K., Shirakabe, K., Shibuya, H., Irie, K., Oishi, I., Ueno, N., Taniguchi, T., Nishida, E., and Matsumoto, K. (1995) *Science* **270,** 2008–2011
9. Kanei-Ishii, C., Ninomiya-Tsuji, J., Tanikawa, J., Nomura, T., Ishitani, T., Kishida, S., Kokura, K., Kurahashi, T., Ichikawa-Iwata, E., Kim, Y., Matsumoto, K., and Ishii, S. (2004) *Genes Dev.* **18,** 816–829
10. Ishitani, T., Kishida, S., Hyodo-Miura, J., Ueno, N., Yasuda, J., Waterman, M., Shibuya, H., Moon, R. T., Ninomiya-Tsuji, J., and Matsumoto, K. (2003) *Mol. Cell. Biol.* **23,** 131–139
11. Hyodo-Miura, J., Urushiyama, S., Nagai, S., Nishita, M., Ueno, N., and Shibuya, H. (2002) *Genes Cells* **7,** 487–496
12. Yamada, M., Ohkawara, B., Ichimura, N., Hyodo-Miura, J., Urushiyama, S., Shirakabe, K., and Shibuya, H. (2003) *Genes Cells* **8,** 677–684
13. Ben-Neriah, Y. (2002) *Nat. Immunol.* **3,** 20–26
14. Bode, A. M., and Dong, Z. (2004) *Nat. Rev. Cancer* **4,** 793–805
15. Fang, S., and Weissman, A. M. (2004) *Cell. Mol. Life Sci.* **61,** 1546–1561
16. Hershko, A., Ciechanover, A., and Varshavsky, A. (2000) *Nat. Med.* **6,** 1073–1081
17. Weissman, A. M. (2001) *Nat. Rev. Mol. Cell. Biol.* **2,** 169–178
18. Freemont, P. S. (2000) *Curr. Biol.* **10,** R84–R87
19. Fang, S., Jensen, J. P., Ludwig, R. L., Vousden, K. H., and Weissman, A. M. (2000) *J. Biol. Chem.* **275,** 8945–8951
20. Honda, R., and Yasuda, H. (2000) *Oncogene* **19,** 1473–1476
21. Joazeiro, C. A., Wing, S. S., Huang, H., Leverson, J. D., Hunter, T., and Liu, Y. C. (1999) *Science* **286,** 309–312
22. Waterman, H., Levkowitz, G., Alroy, I., and Yarden, Y. (1999) *J. Biol. Chem.* **274,** 22151–22154
23. Yokouchi, M., Kondo, T., Houghton, A., Bartkiewicz, M., Horne, W. C., Zhang, H., Yoshimura, A., and Baron, R. (1999) *J. Biol. Chem.* **274,** 31707–31712
24. Huang, H., Joazeiro, C. A., Bonfoco, E., Kamada, S., Leverson, J. D., and Hunter, T. (2000) *J. Biol. Chem.* **275,** 26661–26664
25. Yang, Y., Fang, S., Jensen, J. P., Weissman, A. M., and Ashwell, J. D. (2000) *Science* **288,** 874–877
26. Kamura, T., Koepp, D. M., Conrad, M. N., Skowyra, D., Moreland, R. J., Iliopoulos, O., Lane, W. S., Kaelin, W. G., Jr., Elledge, S. J., Conaway, R. C., Harper, J. W., and Conaway, J. W. (1999) *Science* **284,** 657–661
27. Ohta, T., Michel, J. J., Schottelius, A. J., and Xiong, Y. (1999) *Mol. Cell* **3,** 535–541
28. Seol, J. H., Feldman, R. M., Zachariae, W., Shevchenko, A., Correll, C. C., Lyapina, S., Chi, Y., Galova, M., Claypool, J., Sandmeyer, S., Nasmyth, K., Shevchenko, A., and Deshaies, R. J. (1999) *Genes Dev.* **13,** 1614–1626
29. Gmachl, M., Gieffers, C., Podtelejnikov, A. V., Mann, M., and Peters, J. M. (2000) *Proc. Natl. Acad. Sci. U. S. A.* **97,** 8973–8978
30. Leverson, J. D., Joazeiro, C. A., Page, A. M., Huang, H., Hieter, P., and Hunter, T. (2000) *Mol. Biol. Cell* **11,** 2315–2325
31. Zachariae, W., Shevchenko, A., Andrews, P. D., Ciosk, R., Galova, M., Stark, M. J., Mann, M., and Nasmyth, K. (1998) *Science* **279,** 1216–1219
32. Latres, E., Chiaur, D. S., and Pagano, M. (1999) *Oncogene* **18,** 849–854
33. Winston, J. T., Strack, P., Beer-Romero, P., Chu, C. Y., Elledge, S. J., and Harper, J. W. (1999) *Genes Dev.* **13,** 270–283
34. Tan, P., Fuchs, S. Y., Chen, A., Wu, K., Gomez, C., Ronai, Z., and Pan, Z. Q. (1999) *Mol. Cell* **3,** 527–533
35. Skowyra, D., Koepp, D. M., Kamura, T., Conrad, M. N., Conaway, R. C., Conaway, J. W., Elledge, S. J., and Harper, J. W. (1999) *Science* **284,** 662–665
36. Rupp, R. A., Snider, L., and Weintraub, H. (1994) *Genes Dev.* **8,** 1311–1323
37. Natsume, T., Yamauchi, Y., Nakayama, H., Shinkawa, T., Yanagida, M., Takahashi, N., and Isobe, T. (2002) *Anal. Chem.* **74,** 4725–4733
38. Nishita, M., Hashimoto, M. K., Ogata, S., Laurent, M. N., Ueno, N., Shibuya, H., and Cho, K. W. (2000) *Nature* **403,** 781–785
39. González-Sancho, J. M., Aguilera, O., García, J. M., Pendás-Franco, N., Peña, C., Cal, S., García de Herreros, A., Bonilla, F., and Muñoz, A. (2005) *Oncogene* **24,** 1098–1103

40. Niida, A., Hiroko, T., Kasai, M., Furukawa, Y., Nakamura, Y., Suzuki, Y., Sugano, S., and Akiyama, T. (2004) *Oncogene* **23,** 8520–8526
41. Gay, F., Calvo, D., Lo, M. C., Ceron, J., Maduro, M., Lin, R., and Shi, Y. (2003) *Genes Dev.* **17,** 717–722
42. Sachdev, S., Bruhn, L., Sieber, H., Pichler, A., Melchior, F., and Grosschedl, R. (2001) *Genes Dev.* **15,** 3088–3103
43. Yamamoto, H., Ihara, M., Matsuura, Y., and Kikuchi, A. (2003) *EMBO J.* **22,** 2047–2059
44. Chen, Z., and Pickart, C. M. (1990) *J. Biol. Chem.* **265,** 21835–21842
45. Haldeman, M. T., Xia, G., Kasperek, E. M., and Pickart, C. M. (1997) *Biochemistry* **36,** 10526–10537
46. Lee, S. J., Choi, J. Y., Sung, Y. M., Park, H., Rhim, H., and Kang, S. (2001) *FEBS Lett.* **503,** 61–64
47. Kalchman, M. A., Graham, R. K., Xia, G., Koide, H. B., Hodgson, J. G., Graham, K. C., Goldberg, Y. P., Gietz, R. D., Pickart, C. M., and Hayden, M. R. (1996) *J. Biol. Chem.* **271,** 19385–19394
48. Song, S., Kim, S. Y., Hong, Y. M., Jo, D. G., Lee, J. Y., Shim, S. M., Chung, C. W., Seo, S. J., Yoo, Y. J., Koh, J. Y., Lee, M. C., Yates, A. J., Ichijo, H., and Jung, Y. K. (2003) *Mol. Cell* **12,** 553–563
49. Ohnishi, J., Ohnishi, E., Jin, M., Hirano, W., Nakane, D., Matsui, H., Kimura, A., Sawa, H., Nakayama, K., Shibuya, H., Nagashima, K., and Takahashi, T. (2001) *Mol. Endocrinol.* **15,** 747–764
50. Suzuki, A., Kaneko, E., Maeda, J., and Ueno, N. (1997) *Biochem. Biophys. Res. Commun.* **232,** 153–156

J. Biochem. **139**, 921–930 (2006)
doi:10.1093/jb/mvj104

Proteomic Profiling of Lipid Droplet Proteins in Hepatoma Cell Lines Expressing Hepatitis C Virus Core Protein

Shigeko Sato[1], Masayoshi Fukasawa[1,*], Yoshio Yamakawa[1], Tohru Natsume[2], Tetsuro Suzuki[3], Ikuo Shoji[3], Hideki Aizaki[3], Tatsuo Miyamura[3] and Masahiro Nishijima[1,†]

[1]Department of Biochemistry and Cell Biology and [3]Department of Virology II, National Institute of Infectious Diseases, Tokyo 162-8640; and [2]National Institute of Advanced Industrial Science and Technology (AIST), Biological Information Research Center, Tokyo 135-0064

Received February 7, 2006; accepted April 4, 2006

Hepatitis C virus (HCV) core protein has been suggested to play crucial roles in the pathogeneses of liver steatosis and hepatocellular carcinomas due to HCV infection. Intracellular HCV core protein is localized mainly in lipid droplets, in which the core protein should exert its significant biological/pathological functions. In this study, we performed comparative proteomic analysis of lipid droplet proteins in core-expressing and non-expressing hepatoma cell lines. We identified 38 proteins in the lipid droplet fraction of core-expressing (Hep39) cells and 30 proteins in that of non-expressing (Hepswx) cells by 1-D-SDS-PAGE/MALDI-TOF mass spectrometry (MS) or direct nanoflow liquid chromatography–MS/MS. Interestingly, the lipid droplet fraction of Hep39 cells had an apparently lower content of adipose differentiation–related protein and a much higher content of TIP47 than that of Hepswx cells, suggesting the participation of the core protein in lipid droplet biogenesis in HCV-infected cells. Another distinct feature is that proteins involved in RNA metabolism, particularly DEAD box protein 1 and DEAD box protein 3, were detected in the lipid droplet fraction of Hep39 cells. These results suggest that lipid droplets containing HCV core protein may participate in the RNA metabolism of the host and/or HCV, affecting the pathopoiesis and/or virus replication/production in HCV-infected cells.

Key words: ADRP, DEAD box protein, hepatitis C virus, lipid droplet, TIP47.

Abbreviations: HCV, hepatitis C virus; HCC, hepatocellular carcinoma; MS, mass spectrometry; DNLC, direct nanoflow liquid chromatography; HRP, horseradish peroxidase; ADRP, adipose differentiation–related protein; DDX1, DEAD box protein 1; DDX3, DEAD box protein 3.

Hepatitis C virus (HCV) is a major causative agent of chronic hepatitis (*1*, *2*). Persistent HCV infection, which occurs in more than 70% of infected patients, is strongly associated with the development of liver steatosis, which involves the accumulation of intracellular lipid droplets, cirrhosis, and hepatocellular carcinomas (HCC) (*3*, *4*). Since more than 170 million people in the world are currently infected with HCV (*1*), and there is no cure that is completely effective, understanding the mechanism by which HCV induces serious liver diseases is one of the most important global public health issues. HCV, a member of the *Flaviviridae* family, possesses a single-stranded, positive-sense RNA genome of ~9.6 kb (*5*). The HCV genome has a single open reading frame that codes for a large precursor polyprotein of ~3,000 amino acids that is processed into at least 10 individual proteins by host and viral proteases (*6*).

HCV core protein, the product of the N-terminal portion of the polyprotein, generated upon cleavage at the endoplasmic reticulum by signal peptidase and signal peptide peptidase (*7*, *8*), forms the nucleocapsid of an HCV virion (*9*). Interestingly, in addition to its function as a structural protein, the core protein exhibits activities leading host cells to lipogenic and malignant transformation *in vitro* (*10–12*). Moreover, transgenic mice expressing HCV core protein developed liver steatosis and HCC (*13*, *14*), suggesting an important role of the core protein in these diseases. Many studies have shown that HCV core protein substantially affects various cellular regulatory processes, such as gene transcription (*15–17*) and signal transduction pathways (*12*, *18–23*), and interacts with a variety of host proteins (*12*, *18*, *19*, *22*, *24–34*), but it is not clear what activities/molecules are practically relevant to the pathogeneses of HCV (core)-derived liver steatosis and HCC. Extensive screenings for genes/proteins exhibiting differences in cellular expression by cDNA microarray (*35–40*) or proteome analysis (*41*, *42*) have also been tried for HCV-related HCC. Although various genes/proteins were identified, further studies are required to identify the molecules eventually involved in the pathogenesis of HCV-related HCC.

In host cells, HCV core protein is distributed mainly in lipid droplets and the endoplasmic reticulum (*7*, *10*, *43–46*), in which the core protein is predicted to exert its significant biological/pathological functions. In this study, we thus focused on HCV core protein and lipid droplets, and

*To whom correspondence should be addressed. Tel: +81-3-5285-1111, Fax: +81-3-5285-1157, E-mail: fuka@nih.go.jp
†Present address: Department of Clinical Pharmacy, Faculty of Pharmaceutical Sciences, Doshisha Women's College of Liberal Arts, Kyoto 610-0395.

performed comparative targeted proteomic analysis of the lipid droplet proteins in HCV core–expressing and non-expressing hepatoma cell lines using two strategies: conventional 1-D-SDS-PAGE/MALDI-TOF mass spectrometry (MS) and automated high-throughput direct nanoflow liquid chromatography (DNLC)–MS/MS. We found prominent differences in the protein compositions of lipid droplets between HCV core–expressing and non-expressing hepatoma cell lines.

MATERIALS AND METHODS

Cell Lines—The human hepatoma HepG2 cell line constitutively expressing HCV core protein (Hep39) was established as described previously (*47*). Another HepG2 cell line transfected with expression vector pcEF321swxneo without the HCV core protein insert (Hepswx) was used as a mock control (*47*). Both cell lines were plated on collagen-coated dishes (Asahi Techno Glass, Tokyo, Japan) and maintained in the normal culture medium [DMEM supplemented with 10% fetal bovine serum, 100 units/ml Penicillin G, 100 μg/ml streptomycin sulfate, and 1 mg/ml G418 (Sigma, St. Louis, MO, USA)] under a 5% CO_2 atmosphere at 37°C.

Lipid Droplet Preparation—Hepswx and Hep39 cells were seeded at 4×10^6 cells/dish (150 mm, inner diameter) in 25 ml of normal culture medium and cultured for one day. For efficient formation of lipid droplets by cells, cholesterol (final 20 μg/ml) and oleic acid (final 400 μM)/fatty acid–free BSA (final 60 μM) complex, prepared as stock solutions of 5 mg/ml cholesterol in ethanol and 10 mM oleic acid/1.5 mM BSA in PBS, respectively, were added to the medium. Each cell line was further incubated for 48–72 h at 37°C. For proteomic analysis of lipid droplet proteins, confluent monolayers of Hepswx and Hep39 cells in fifteen cell culture dishes (150 mm, inner diameter) were harvested by scraping and pelleted by centrifugation ($200 \times g$ for 5 min at 4°C). After being washed with PBS three times, each cell pellet was resuspended in 10 mM Tris-HCl buffer, pH 7.5, containing 0.25 M sucrose and Complete™, EDTA-free (Roche, Mannheim, Germany) to achieve a final volume equal to five times the volume of the cell pellet (*i.e.* a 20% cell suspension). The cell suspension was homogenized with a ball-bearing homogenizer (*48*), and then centrifuged at $800 \times g$ for 5 min at 4°C. One milliliter of each post-nuclear supernatant fraction was layered under 2 ml of 10 mM Tris-HCl buffer, pH 7.5, containing 0.15 M NaCl (TN-buffer). After centrifugation at $100{,}000 \times g$ for 60 min at 4°C, the lipid droplet fraction, *i.e.* the distinct white band on the top of the preparation, was collected with a pipetman. The floating lipid droplet fraction was diluted with 3.5 ml of TN-buffer and then re-purified by centrifugation ($100{,}000 \times g$ for 30 min at 4°C). This washing step was repeated three times. Lipid droplets in the floating fractions in both cells were enriched up to more than 500-fold compared with those in the total cell lysates as estimated by their protein contents. The amounts of lipid droplets isolated from Hepswx and Hep39 cells were nearly the same. The purified lipid droplet fractions (~0.1 mg of protein per ml) were stored at −80°C until use. The purity of the lipid droplet fractions was verified by microscopic and immunoblot (Fig. 1) analyses. Adipose differentiation–related protein (ADRP), a known lipid droplet protein, was significantly enriched in the lipid droplet fractions of Hepswx and Hep39 cells (Fig. 1). Other organelle marker proteins, such as nucleoporin p62 for the nucleus, prohibitin for the mitochondria, fatty acid synthase for the cytoplasm, GM130 for the Golgi apparatus, EEA1 for the early endosome, or annexin II for the plasma membrane, were not detected in the lipid droplet fractions of either cells (Fig. 1). Small amounts of calnexin, a marker of the endoplasmic reticulum, which is a major organelle, were detected in the lipid droplet fractions of both cells to a similar extent. Although we did not detect calnexin in the lipid droplet fractions by proteomic analysis (see Tables 1 and 2), the lipid droplet fractions of both cells could be contaminated with a small amount of endoplasmic reticulum.

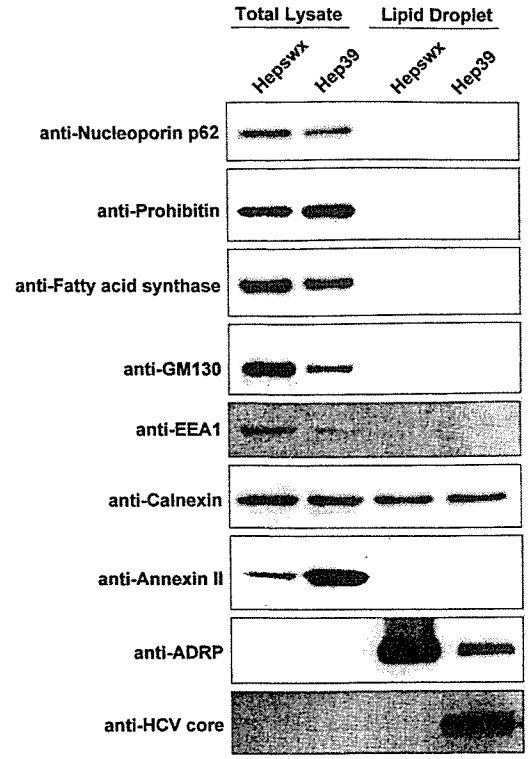

Fig. 1. **Immunoblot analysis of lipid droplet fractions in Hepswx and Hep39 cells using antibodies against various organelle markers.** Total cell lysates and lipid droplet fractions (1.5 μg of protein per lane in the case of anti-ADRP; 5 μg of protein per lane in others) from Hepswx and Hep39 cells were analyzed by immunoblotting with the indicated antibodies.

1-D-SDS-PAGE/MALDI-TOF MS Analysis—The lipid droplet fraction (30 μg protein) of each cell line was fractionated in a 10% SDS–polyacrylamide gel, and the gel was stained with Coomassie Brilliant Blue. The protein bands were excised from the gel and subjected to in-gel trypsin digestion. The tryptic peptide mixtures were analyzed by MALDI-TOF MS as described previously (*49*). Prior to MALDI-TOF MS analysis, the peptide mixtures were desalted using C18 Zip Tips (Millipore, Billerica, MA, USA) according to the manufacturer's instructions. The peptide data were collected in the reflection mode and with positive polarity, using a saturated solution of

Table 1. **Lipid droplet proteins identified in Hepswx and Hep39 cells by means of 1-D-SDS-PAGE/MALDI-TOF MS.**

Protein	Molecular mass (kDa) (calc.)	Accession No.	SDS band No.[a]	
			Hepswx	Hep39
PAT family proteins				
Adipose differentiation–related protein (ADRP)	48.1	34577059	5	21
Cargo selection protein/TIP47	47.0	20127486		22
Lipid metabolism				
Acyl CoA synthetase long chain family member 3	80.4	42794752	4	18
Cytochrome b_5 reductase	34.3	4503327	9	26
Lanosterol synthase	83.3	4808278	4	18
NAD(P)-dependent steroid dehydrogenase-like; H105e3	41.9	8393516	8	25
Retinal short-chain dehydrogenase/reductase retSDR2	33.0	7705905	10	27
Cytosolic phospholipase A_2	85.2	1352707		14
Rab GTPases				
Rab1A	22.7	4758988	13	30
Rab1B	22.2	23396834	13	30
Rab5C	23.5	38258923	11	28
Rab7	23.5	34147513	12	29
RNA metabolism/binding				
DEAD box protein 1 (DDX1)	82.9	6919862		16
DEAD box protein 3 (DDX3)	73.2	3023628		18
HC56/gemin 4	118.8	10945430		15
Other/unknown proteins				
BiP protein	70.9	14916999	3	17
CGI-49 protein	46.9	7705767	6	23
Heat shock protein gp96 precursor	90.2	15010550	2	14
Ancient ubiquitous protein 1	41.4	31712024	7	
Major vault protein	99.3	15990478	1	
Apoptosis-inducing factor–homologous mitochondrion-associated inducer of death	40.5	13543964		24
KIAA0887 protein	52.4	4240263		21
Protein disulfide-isomerase [EC 5.3.4.1] ER60 precursor	56.7	1085373		20
Transport-secretion protein 2.1	57.7	9663151		19
HCV core protein	20.6	974345		31

[a]Band numbers correspond to those in Fig. 2.

α-cyano-4-hydroxycinnamic acid (Sigma) in 50% acetonitrile and 0.1% trifluoroacetic acid as the matrix. Spectra were obtained using a Voyager DE-STR MALDI-TOF mass spectrometer (PE Biosystems, Foster City, CA, USA). Internal calibration was performed with adrenocorticotropic hormone, fragment 18–39 (Sigma), and bradykinin fragment (Sigma). The data base–fitting program MS-Fit available at the WWW site of the University of California, San Francisco (prospector.ucsf.edu/ucsfhtml3.4/msfit.htm) was used to interpret the MS spectra of protein digests (*50*).

DNLC-MS/MS Analysis—The lipid droplet fraction (10 μg protein) of each cell line was first delipidated by chloroform–methanol extraction as originally described (*51*). Two volumes of chloroform and 1 volume of methanol were mixed with 0.8 volume of the lipid droplet fraction. Then, 1 volume of chloroform and 1 volume of water were added to the mixture, and the mixture was vortexed for 30 s, and centrifuged at 10,000 × *g* for 5 min at room temperature. The resulting organic (lower) phase was removed. The aqueous (upper) phase and interface, containing all the lipid droplet proteins, was lyophilized. The delipidated lipid droplet proteins were digested with endoproteinase Lys-C, and the resulting peptides were analyzed by DNLC-MS/MS as described (*52*, *53*).

Cell Fractionation—All manipulations were performed at 4°C or on ice. After being washed with PBS, confluent monolayers of Hepswx and Hep39 cells were harvested by scraping and pelleted by centrifugation (200 × *g*, 5 min). The precipitated cells were homogenized with a ball-bearing homogenizer in 10 mM Tris-HCl buffer, pH 7.5, containing 0.25 M sucrose, and Complete™, EDTA-free. After centrifugation of the lysate at 800 × *g* for 5 min, the cytosolic fraction (100,000 × *g* supernatant) and membrane fraction (100,000 × *g* precipitate) were separated from the post-nuclear supernatant fraction by centrifugation at 100,000 × *g* for 60 min. The membrane fraction was resuspended in TN-buffer and then re-purified twice by centrifugation. The protein concentrations of these preparations were determined with BCA protein assay reagents (Pierce Biotechnology, Rockford, IL, USA) using BSA as a standard.

Immunoblot Analysis—Equivalent amounts of proteins from Hepswx and Hep39 cells were separated in a 10 or 12.5% SDS–polyacrylamide gel and then electrophoretically transferred to a polyvinylidene difluoride membrane. The membranes were blocked overnight at 4°C or 30 min at room temperature in TBS containing 0.1% Tween 20 and 5% skim milk. The blots were probed with a mouse

Table 2. **Lipid droplet proteins identified in Hepswx and Hep39 cells by means of DNLC-MS/MS.**

Protein	Accession No.	Molecular mass (kDa) (calc.)	Matched peptide sequence	
			Hepswx[a]	Hep39[a]
PAT family proteins				
Adipose differentiation–related protein (ADRP)	34577059	48.1	+ TITSVAMTSALPIIQK DAVTTTVTGAK EVSDSLLTSSK	+ TITSVAMTSALPIIQK DAVTTTVTGAK EVSDSLLTSSK
Cargo selection protein / TIP47	20127486	47.0	+ VSGAQEMVSSAK	+ VSGAQEMVSSAK
Lipid metabolism				
Acyl-CoA synthetase long-chain family member 3	42794752	80.4	+ VLSEAAISASLEK	+ ELTELARK
Cytochrome b_5 reductase	4503327	34.2	+ DILLRPELEELRNK	+ SNPIIRTVK
Gastric-associated differentially-expressed protein YA61P	6970062	14.9	+ AIGLVVPSLTGK	+ AIGLVVPSLTGK
Retinal short-chain dehydrogenase/ reductase retSDR2	7705905	33.0	+ HGLEETAAK	+ FDAVIGYK
Sterol carrier protein 2–related form, 58.85K	86717	58.8	+ LQNLQLQPGNAK	+ LQNLQLQPGNAK
Acyl-CoA synthetase long-chain family member 4	4758332	74.4	+ SDQSYVISFVVPNQK	
Fatty acid binding protein 5	4557581	15.2	+ ELGVGIALRK	
Hydroxysteroid (17-beta) dehydrogenase 4	4504505	79.7		+ NHPMTPEAVK
Rab GTPases				
Rab1A	4758988	22.6	+[b] QWLQEIDRYASENVNK RMGPGATAGGAEK	+ RMGPGATAGGAEK
Rab1B	23396834	22.1	+[b] QWLQEIDRYASENVNK	+ RMGPGAASGGERPNLK
Rab7	34147513	23.5	+ NNIPYFETSAK	+ ATIGADFLTK
Rab18	20809384	22.9	+ HSMLFIEASAK	+ ILIIGESGVGK
Rab10	12654157	22.5	+ LLLIGDSGVGK	
Rab11	4758986	24.5	+ VVLIGDSGVGK	
Rab8	539607	23.6		+ IRTIELDGK
RNA metabolism/binding				
DEAD box protein 1 (DDX1)	6919862	82.4		+ FGFGFGGTGK
DEAD box protein 3 (DDX3)	3023628	73.2		+ GVRHTMMFSATFPK
IGF-II mRNA-binding protein 3	30795212	63.7		+ EGATIRNITK
Ribosomal protein L29	14286258	17.8		+ AQAAAPASVPAQAPK
Other/unknown proteins				
Apoptosis-inducing factor homologous mitochondrion-associated inducer of death	13543964	40.5	+ EVTLIHSQVALADK	+ EVTLIHSQVALADK
BiP protein	14916999	72.3	+ SQIFSTASDNQPTVTIK	+ VYEGERPLTK
Hypothetical protein DKFZp586A0522.1	7512845	28.2	+ LQHIQAPLSWELVRPH-IYGYAVK	+ RELFSNLQEFAGPSGK
Prolyl 4-hydroxylase, beta subunit	20070125	57.1	+ VHSFPTLK	+ AEGSEIRLAK
Ancient ubiquitous protein 1	31712024	41.4	+ GTQSLPTASASK	
Heat shock protein gp96 precursor	15010550	90.2	+ FAFQAEVNRMMK	
Hypothetical protein FLJ21820	11345458	37.3	+ DIYGLNGQIEHK	
Molecule possessing ankyrin repeats induced by lipopolysaccharide	38173790	78.1	+ CLIQMGAAVEAK	
Ubiquitin-conjugating enzyme E2G 2, isoform 1	15079469	18.6	+ RLMAEYK	
CGI-49 protein	7705767	46.9		+ AGGVFTPGAAFSK
DILV594	37182139	31.4		+ RELFSQIK
Hypothetical protein DKFZp564F0522.1—human (fragment)	7512734	33.1		+ ILRTSSGSIREK
Hypothetical protein HSPC117	7657015	55.2		+ EQLAQAMFDHIPVGVGSK
Tumor protein D52–like 2 isoform e	40805860	22.2		+ TQETLSQAGQK
Vesicle amine transport protein 1	15679945	41.9		+ VVTYGMANLLTGPK

[a]+, detected. [b]This peptide sequence is present in both Rab1A and Rab1B.

monoclonal anti-ADRP antibody (PROGEN Biotechnik GmbH, Heidelberg, Germany) (1:25), a guinea pig polyclonal anti-TIP47 antibody (PROGEN Biotechnik GmbH) (1:250), a mouse monoclonal anti-HCV core protein antibody (Anogen, Ontario, Canada) (1: 1,000), a mouse monoclonal anti-DDX1 antibody (Pharmingen, San Diego, CA, USA) (1:500), or a rabbit polyclonal anti-DDX3 antibody (antibody custom-made by Invitrogen, CA, USA) (1:500) for 90 min at room temperature. The blots were then incubated with horseradish peroxidase (HRP)–conjugated goat anti-rabbit IgG (BIO-RAD), HRP-conjugated goat anti-mouse IgG (BIO-RAD), or HRP-conjugated goat anti-guinea pig IgG (ICN Pharmaceuticals, Aurora, OH, USA) at 1:2,000 dilution for 60 min. Detection of immunoreactive proteins was performed with an ECL system (Amersham Biosciences Corp., Piscataway, NJ, USA).

RESULTS

Proteomic Analysis of Lipid Droplets by 1-D-SDS-PAGE/MALDI-TOF MS—Lipid droplet proteins from control (HCV core non-expressing) Hepswx cells and HCV core–expressing Hep39 cells were separated by 10% SDS-PAGE, and the protein bands were visualized by Coomassie Brilliant Blue staining (Fig. 2). In each cell line ~30 bands were seen. The visible bands (areas) were excised from the gels, trypsinized, and analyzed by MALDI-TOF MS. Among the 31 bands, we identified 25 proteins: 15 proteins in Hepswx cells and 23 proteins in Hep39 cells (Fig. 2 and Table 1). Thirteen of the 25 proteins were detected in both types of cell. The lipid droplet proteins found in both Hepswx and Hep39 cells could be categorized into four groups: (1) PAT family proteins, *i.e.* ADRP and TIP47; (2) multiple molecules involved in lipid metabolism; (3) several Rab GTPases; and (4) other/unknown proteins (Table 1). In addition, Hep39 cells contained another group of proteins involved in RNA metabolism/binding (Table 1).

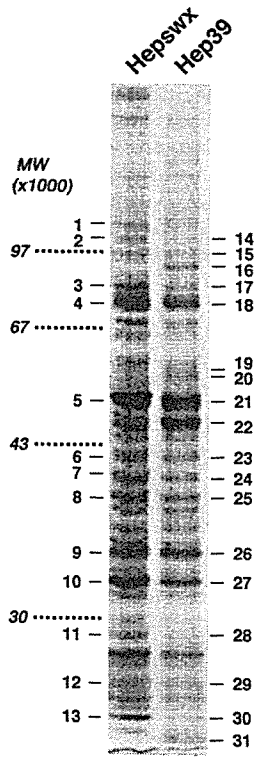

Fig. 2. **Signature SDS-PAGE patterns of the lipid droplet fractions of Hepswx and Hep39 cells.** Proteins in the purified lipid droplet fractions (30 μg of protein per lane) of Hepswx cells and Hep39 cells were separated in a 10% SDS–polyacrylamide gel, and visualized by Coomassie Brilliant Blue staining. The 31 numbered bands were excised from the gel, subjected to in-gel trypsin digestion, and processed for MALDI-TOF-MS. Molecular weights (MW) are given to the left of the gel.

Proteomic Analysis of Lipid Droplets by DNLC-MS/MS—Some protein bands in Fig. 2 could not be identified, probably due to the restricted separation capacity of 1-D-SDS-PAGE (*i.e.* multiple proteins migrating to the same area). We had, however, difficulty in applying 2-DE to the separation of lipid droplet proteins because of their hydrophobic characteristics. We then tried a new LC-based MS strategy. Lipid droplet fractions from Hepswx and Hep39 cells were delipidated and then digested with Lys-C. The resulting peptide mixtures were directly analyzed using a DNLC-MS/MS system (*52*). We identified 36 lipid droplet proteins: 24 proteins in Hepswx cells and 27 proteins in Hep39 cells (Table 2). Twenty-three lipid droplet proteins were newly identified with this system. Fifteen proteins detected in both cell lines were classified into four categories (Table 2) as in the case of 1-D-SDS-PAGE/MALDI-TOF MS analysis. A group of proteins involved in RNA metabolism/binding was also found only in Hep39 cells (Table 2).

Proteins Exhibiting Differences in Their Association with Lipid Droplets Due to HCV Core Protein Expression—SDS-PAGE patterns of lipid droplet proteins were similar but revealed several distinct differences in protein composition between Hepswx and Hep39 cells (Fig. 2). The most remarkable differences were seen in the bands corresponding to PAT family proteins. The amount of ADRP, a major PAT family protein in lipid droplets in the liver (*54*, *55*), and likely to be the most abundant lipid droplet protein in Hepswx cells (Fig. 2, band 5), seemed to be less in HCV core–expressing Hep39 cells (Fig. 2, band 21). On the other hand, TIP47, which is also known to be a PAT family protein in lipid droplets (*56*, *57*), was detected as a major protein only in Hep39 cells (Fig. 2, band 22, and Table 1). To confirm these findings, the contents of ADRP and TIP47 in the lipid droplet fractions of Hepswx and Hep39 cells were examined by immunoblot analysis with specific antibodies. The lipid droplet fraction of HCV core–expressing Hep39 cells showed an apparently lower content of ADRP and a much higher content of TIP47 than the levels in Hepswx cells (Fig. 3).

Next we examined the cellular distributions of ADRP and TIP47 in Hepswx and Hep39 cells by cell fractionation. ADRP was highly concentrated in the lipid droplet fractions of both cells, even though the content in the lipid droplets was much lower in Hep39 cells than in Hepswx cells (Fig. 4). ADRP was not detected in post-nuclear supernatant fractions or in either the cytosol or membrane fractions, probably because of low expression levels in these cells or low affinity of the anti-ADRP antibody we used

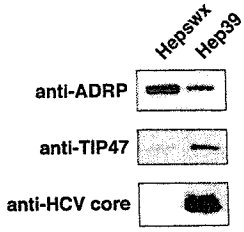

Fig. 3. **The lipid droplet fraction of Hep39 cells contains less ADRP, but more TIP47, than Hepswx cells.** Lipid droplet fractions (1.5 μg of protein per lane) from Hepswx and Hep39 cells were analyzed by immunoblotting with the indicated antibodies.

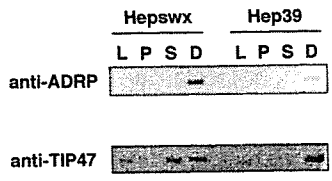

Fig. 4. **Subcellular localization of ADRP and TIP47 in Hepswx and Hep39 cells.** Hepswx and Hep39 cells were fractionated into post-nuclear supernatant (lane L), 100,000 × *g* precipitate (lane P), 100,000 × *g* supernatant (lane S), and lipid droplet (lane D) fractions as described in "MATERIALS AND METHODS." Ten micrograms of protein was processed for gel electrophoresis, and then analyzed by immuonoblotting with anti-ADRP and anti-TIP47 antibodies.

(Fig. 4). The mRNA expression level of ADRP in Hep39 cells was less than half that in Hepswx cells (data not shown), consistent with the immunoblot data shown in Fig. 4. These results suggest that the lower ADRP content in the lipid droplet fraction of Hep39 cells is due to a low expression level of ADRP. In contrast, Hep39 cells had much more TIP47 in the lipid droplet fraction (Figs. 3 and 4, lanes D), but the cellular TIP47 content of Hep39 cells was not more than that in Hepswx cells (Fig. 4, lanes L). Besides the lipid droplet fraction, the cytosolic fraction of Hepswx cells was found to contain TIP47 at a substantial level, while the cytosolic fraction of Hep39 cells did not (Fig. 4, lanes S). These results indicate that the intracellular distribution of TIP47 shifts drastically from the cytosol to lipid droplets in HCV core–expressing Hep39 cells.

Another obvious difference between Hepswx and Hep39 cells in Fig. 2 is the presence of a specific ~85 kDa band (Fig. 2, band 16) in Hep39 cells, which was identified as DEAD box protein 1 (DDX1), a DEAD box protein family member, by 1-D-SDS-PAGE/MALDI-TOF MS analysis (Table 1). DNLC-MS/MS analysis also supported the existence of DDX1 in the lipid droplet fraction of Hep39 cells (Table 2). In addition, DEAD box protein 3 (DDX3), another DEAD box protein family member, was also detected in the lipid droplet fraction of Hep39 cells by means of the two different strategies used for proteomic analysis (Tables 1 and 2), suggesting that DDX3 is a major lipid droplet protein in Hep39 cells. To verify the association of DDX 1 and DDX3 with lipid droplets in Hep39 cells, immunoblot analysis was carried out. Figure 5 shows that DDX 1 and DDX 3 exist in the lipid droplet fraction of HCV core-expressing Hep39 cells, but not Hepswx cells. These results imply the

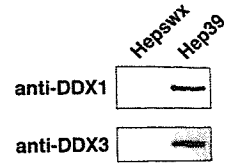

Fig. 5. **Hep39 cells, but not Hepswx cells, have DDX1 and DDX3 in the lipid droplet fraction.** Lipid droplet fractions (0.5 μg of protein per lane) in Hepswx and Hep39 cells were analyzed by immunoblotting with anti-DDX1 and anti-DDX3 antibodies.

special pathological functions of DDX1 and DDX3 in lipid droplets in HCV core–expressing cells.

DISCUSSION

To analyze lipid droplet proteins, we performed proteomic analysis by means of 1-D-SDS-PAGE/MALDI-TOF MS and automated DNLC-MS/MS, and identified 25 and 36 proteins, respectively (Tables 1 and 2). Many more lipid droplet proteins were identified by DNLC-MS/MS, and 22 major proteins separated by 1-D-SDS-PAGE (Fig. 2, bands, 2, 3, 4, 5, 7, 9, 10, 12, 13, 16, 17, 18, 21, 22, 24, 26, 27, 29, and 30) and detected on MALDI-TOF MS analysis were also detected on DNLC-MS/MS analysis. These results indicate that DNLC-MS/MS is a very sensitive and reliable system as well as a high-throughput method. Particularly, DNLC-MS/MS would be a powerful system for exhaustive proteomic analysis of protein mixtures/complexes (up to ~100 proteins) such as lipid droplets.

In our targeted proteomic study, we identified a total of 48 lipid droplet proteins: 30 proteins in control Hepswx cells, 38 proteins in HCV core–expressing Hep39 cells, and 20 proteins in both cell lines. The resident lipid droplet proteins were classified into four groups (Tables 1 and 2), consistent with the recently reported data obtained on proteomic analysis of lipid droplet proteins in other cell lines (*58–60*). In addition, multiple proteins, such as the sterol carrier protein 2–related form, fatty acid binding protein 5, and apoptosis-inducing factor homologous mitochondrion-associated inducer of death, were newly identified as lipid droplet proteins in this study. These accumulated data obtained on proteomic analysis will be useful for understanding the biogenesis and functions of lipid droplets about which little is yet known.

A prominent effect of the expression of HCV core protein on the composition of lipid droplet proteins was observed among the PAT family proteins, i.e. ADRP and TIP47. HCV core–expressing Hep39 cells contained much less ADRP in the lipid droplet fraction (Fig. 3), probably because of the lower cellular expression level and the lack of induction of expression upon lipid loading (data not shown). In contrast, a substantial amount of TIP47 was associated with the lipid droplet fraction of Hep39 cells (Fig. 3). Perilipin, a structural protein of lipid droplets in adipocytes, ADRP, and TIP47, termed PAT family proteins (*61*), share extensive amino acid sequence similarity (*61–63*), suggesting a common biological function in lipid droplet formation. For example, the transition in surface protein composition of lipid droplets from ADRP to perilipin occurs during adipocyte differentiation (*64*). Thus, TIP47 might replace ADRP

on the lipid droplets in Hep39 cells. Cellular TIP47 was not up-regulated in Hep39 cells, resulting in a reduction of TIP47 in the cytosolic fraction (Fig. 4). Since TIP47, originally identified as having the ability to interact with the mannose 6-phosphate/IGF-II receptor (*63*), appears to be essential for the endocytic recycling system (*65–67*), the altered distribution of cellular TIP47 in Hep39 cells could affect intracellular membrane trafficking pathways. Consistent with this assumption, our preliminary results showed that the rate of protein secretion from cells was apparently slower for Hep39 cells than Hepswx cells (unpublished data). Patients chronically infected with HCV (*68*) and HCV core–transgenic mice (*69*) exhibit decreased levels of plasma very low density lipoproteins secreted from the liver, also suggesting interference with intracellular membrane trafficking (secretion pathways) by HCV core proteins. We currently speculate that the reduction in cellular ADRP expression mediated by HCV core protein causes the accumulation of TIP47 in lipid droplets as a substitute, and that the resulting depletion of TIP47 in the cytosol could cause the impairment of intracellular membrane trafficking, followed by the cellular accumulation of membrane lipids and consequent lipid droplet formation. Although further studies remain to be done to confirm these possibilities, we suggest that HCV core protein influences not only the biogenesis of lipid droplets but also intracellular membrane trafficking.

Another interesting finding in this study is that Hep39 cells, unlike Hepswx cells, contain DEAD box proteins, DDX1 and DDX3, as major lipid droplet proteins (Figs. 2 and 5). On the basis of the results of studies involving yeast two-hybrid assays, DDX3 has been shown to be able to interact with HCV core protein, and studies involving immunofluorescent microscopy have revealed that DDX3 is distributed in cytosolic spots such as lipid droplets (*27, 70, 71*). These results, together with our present findings, suggest that DDX3 is associated with lipid droplets via HCV core proteins located on lipid droplets. In addition to DDX1 and DDX3, which possess ATPase/RNA helicase activities (*27, 72, 73*), several other proteins involved in RNA metabolism/binding, including HC56/gemin 4 and IGF-II mRNA–binding protein 3, were also detected in the lipid droplet fraction of HCV core-expressing Hep39 cells (Tables 1 and 2). Recently Dvorak *et al.* reported that RNA itself can be associated with lipid droplets in human mast cells (*74*). Taken together, these data strongly suggest that lipid droplets containing HCV core proteins may participate in the RNA metabolism of the host and/or HCV in HCV-infected cells. Furthermore, the findings that DDX1 is overexpressed in cell lines derived from tumors such as retinoblastomas and neuroblastomas (*75*), and that cellular expression of DDX3 induces anchorage-independent cell growth (*76*) suggest the involvement of DDX1 and DDX3 in carcinogenesis.

Some groups recently reported profiles of mRNAs up- or down-regulated by expression of the HCV core protein (*77–79*), but these mRNAs included no molecules identified as lipid droplet proteins in this study. Since lipid droplets are a minor organelle in cells, it might be difficult to detect changes in the mRNA expression levels of lipid droplet proteins. The merits of targeted proteomic study are that it is possible to focus on minor cellular fractions, and also to detect changes in the intracellular distributions of proteins. Actually, the mRNA expression levels of TIP47, DDX1, and DDX3 did not change in Hep39 cells (data not shown).

We identified many other lipid droplet proteins found in either Hepswx or Hep39 cells, but their biological functions remain mostly unknown (Tables 1 and 2). Elucidation of the biological functions of these proteins will lead to an advanced understanding of the pathogeneses of HCV-derived liver diseases.

This work was supported by Grants-in-Aid from the Ministry of Health, Labor and Welfare; the program for the Promotion of Fundamental Studies in Health Sciences of the Organization for Drug ADR Relief, R&D Promotion, and Product Review of Japan; the TAKEDA SCIENCE FOUNDATION; and the Integrated Proteomics System Project for Pioneer Research on Genome the Frontier from the Ministry of Education, Culture, Sports, Science & Technology of Japan.

REFERENCES

1. Choo, Q.L., Kuo, G., Weiner, A.J., Overby, L.R., Bradley, D.W., and Houghton, M. (1989) Isolation of a cDNA clone derived from a blood-borne non-A, non-B viral hepatitis genome. *Science* **244**, 359–362
2. Kuo, G., Choo, Q.L., Alter, H.J., Gitnick, G.L., Redeker, A.G., Purcell, R.H., Miyamura, T., Dienstag, J.L., Alter, M.J., Stevens, C.E., Tegtmeier, G.E., Bonino, F., Colombo, M., Lee, W.-S., Kuo, C., Berger, K., Shuster, J.R., Overby, L.R., Bradley, D.W., and Houghton, M. (1989) An assay for circulating antibodies to a major etiologic virus of human non-A, non-B hepatitis. *Science* **244**, 362–364
3. Saito, I., Miyamura, T., Ohbayashi, A., Harada, H., Katayama, T., Kikuchi, S., Watanabe, Y., Koi, S., Onji, M., Ohta, Y., Choo, Q.-L., Houghton, M., and Kuo, G. (1990) Hepatitis C virus infection is associated with the development of hepatocellular carcinoma. *Proc. Natl. Acad. Sci. USA* **87**, 6547–6549
4. Kiyosawa, K., Sodeyama, T., Tanaka, E., Gibo, Y., Yoshizawa, K., Nakano, Y., Furuta, S., Akahane, Y., Nishioka, K., Purcell, R.H., and Alter, H.J. (1990) Interrelationship of blood transfusion, non-A, non-B hepatitis and hepatocellular carcinoma: analysis by detection of antibody to hepatitis C virus. *Hepatology* **12**, 671–675
5. Bartenschlager, R. and Lohmann, V. (2000) Replication of hepatitis C virus. *J. Gen. Virol.* **81**, 1631–1648
6. Grakoui, A., Wychowski, C., Lin, C., Feinstone, S.M., and Rice, C.M. (1993) Expression and identification of hepatitis C virus polyprotein cleavage products. *J. Virol.* **67**, 1385–1395
7. McLauchlan, J., Lemberg, M.K., Hope, G., and Martoglio, B. (2002) Intramembrane proteolysis promotes trafficking of hepatitis C virus core protein to lipid droplets. *EMBO J.* **21**, 3980–3988
8. Okamoto, K., Moriishi, K., Miyamura, T., and Matsuura, Y. (2004) Intramembrane proteolysis and endoplasmic reticulum retention of hepatitis C virus core protein. *J. Virol.* **78**, 6370–6380
9. Santolini, E., Migliaccio, G., and La Monica, N. (1994) Biosynthesis and biochemical properties of the hepatitis C virus core protein. *J. Virol.* **68**, 3631–3641
10. Barba, G., Harper, F., Harada, T., Kohara, M., Goulinet, S., Matsuura, Y., Eder, G., Schaff, Z., Chapman, M.J., Miyamura, T., and Brechot, C. (1997) Hepatitis C virus core protein shows a cytoplasmic localization and associates to cellular lipid storage droplets. *Proc. Natl. Acad. Sci. USA* **94**, 1200–1205
11. Ray, R.B., Lagging, L.M., Meyer, K., and Ray, R. (1996) Hepatitis C virus core protein cooperates with ras and transforms

primary rat embryo fibroblasts to tumorigenic phenotype. *J. Virol.* **70**, 4438–4443
12. Yoshida, T., Hanada, T., Tokuhisa, T., Kosai, K., Sata, M., Kohara, M., and Yoshimura, A. (2002) Activation of STAT3 by the hepatitis C virus core protein leads to cellular transformation. *J. Exp. Med.* **196**, 641–653
13. Moriya, K., Yotsuyanagi, H., Shintani, Y., Fujie, H., Ishibashi, K., Matsuura, Y., Miyamura, T., and Koike, K. (1997) Hepatitis C virus core protein induces hepatic steatosis in transgenic mice. *J. Gen. Virol.* **78**, 1527–1531
14. Moriya, K., Fujie, H., Shintani, Y., Yotsuyanagi, H., Tsutsumi, T., Ishibashi, K., Matsuura, Y., Kimura, S., Miyamura, T., and Koike, K. (1998) The core protein of hepatitis C virus induces hepatocellular carcinoma in transgenic mice. *Nat. Med.* **4**, 1065–1067
15. Kim, D.W., Suzuki, R., Harada, T., Saito, I., and Miyamura, T. (1994) Trans-suppression of gene expression by hepatitis C viral core protein. *Jpn. J. Med. Sci. Biol.* **47**, 211–220
16. Ray, R.B., Steele, R., Meyer, K., and Ray, R. (1997) Transcriptional repression of p53 promoter by hepatitis C virus core protein. *J. Biol. Chem.* **272**, 10983–10986
17. Shrivastava, A., Manna, S.K., Ray, R., and Aggarwal, B.B. (1998) Ectopic expression of hepatitis C virus core protein differentially regulates nuclear transcription factors. *J. Virol.* **72**, 9722–9728
18. Chen, C.M., You, L.R., Hwang, L.H., and Lee, Y.H. (1997) Direct interaction of hepatitis C virus core protein with the cellular lymphotoxin-beta receptor modulates the signal pathway of the lymphotoxin-beta receptor. *J. Virol.* **71**, 9417–9426
19. Zhu, N., Khoshnan, A., Schneider, R., Matsumoto, M., Dennert, G., Ware, C., and Lai, M.M. (1998) Hepatitis C virus core protein binds to the cytoplasmic domain of tumor necrosis factor (TNF) receptor 1 and enhances TNF-induced apoptosis. *J. Virol.* **72**, 3691–3697
20. Tsuchihara, K., Hijikata, M., Fukuda, K., Kuroki, T., Yamamoto, N., and Shimotohno, K. (1999) Hepatitis C virus core protein regulates cell growth and signal transduction pathway transmitting growth stimuli. *Virology* **258**, 100–107
21. You, L.R., Chen, C.M., and Lee, Y.H. (1999) Hepatitis C virus core protein enhances NF-kappaB signal pathway triggering by lymphotoxin-beta receptor ligand and tumor necrosis factor alpha. *J. Virol.* **73**, 1672–1681
22. Aoki, H., Hayashi, J., Moriyama, M., Arakawa, Y., and Hino, O. (2000) Hepatitis C virus core protein interacts with 14–3-3 protein and activates the kinase Raf-1. *J. Virol.* **74**, 1736–1741
23. Yoshida, H., Kato, N., Shiratori, Y., Otsuka, M., Maeda, S., Kato, J., and Omata, M. (2001) Hepatitis C virus core protein activates nuclear factor kappa B-dependent signaling through tumor necrosis factor receptor-associated factor. *J. Biol. Chem.* **276**, 16399–16405
24. Matsumoto, M., Hsieh, T.Y., Zhu, N., VanArsdale, T., Hwang, S.B., Jeng, K.S., Gorbalenya, A.E., Lo, S.Y., Ou, J.H., Ware, C.F., and Lai, M.M. (1997) Hepatitis C virus core protein interacts with the cytoplasmic tail of lymphotoxin-beta receptor. *J. Virol.* **71**, 1301–1309
25. Hsieh, T.Y., Matsumoto, M., Chou, H.C., Schneider, R., Hwang, S.B., Lee, A.S., and Lai, M.M. (1998) Hepatitis C virus core protein interacts with heterogeneous nuclear ribonucleoprotein K. *J. Biol. Chem.* **273**, 17651–17659
26. Sabile, A., Perlemuter, G., Bono, F., Kohara, K., Demaugre, F., Kohara, M., Matsuura, Y., Miyamura, T., Brechot, C., and Barba, G. (1999) Hepatitis C virus core protein binds to apolipoprotein AII and its secretion is modulated by fibrates. *Hepatology* **30**, 1064–1076
27. You, L.R., Chen, C.M., Yeh, T.S., Tsai, T.Y., Mai, R.T., Lin, C.H., and Lee, Y.H. (1999) Hepatitis C virus core protein interacts with cellular putative RNA helicase. *J. Virol.* **73**, 2841–2853
28. Jin, D.Y., Wang, H.L., Zhou, Y., Chun, A.C., Kibler, K.V., Hou, Y.D., Kung, H., and Jeang, K.T. (2000) Hepatitis C virus core protein-induced loss of LZIP function correlates with cellular transformation. *EMBO J.* **19**, 729–740
29. Wang, F., Yoshida, I., Takamatsu, M., Ishido, S., Fujita, T., Oka, K., and Hotta, H. (2000) Complex formation between hepatitis C virus core protein and p21Waf1/Cip1/Sdi1. *Biochem. Biophys. Res. Commun.* **273**, 479–484
30. Otsuka, M., Kato, N., Lan, K., Yoshida, H., Kato, J., Goto, T., Shiratori, Y., and Omata, M. (2000) Hepatitis C virus core protein enhances p53 function through augmentation of DNA binding affinity and transcriptional ability. *J. Biol. Chem.* **275**, 34122–34130
31. Tsutsumi, T., Suzuki, T., Shimoike, T., Suzuki, R., Moriya, K., Shintani, Y., Fujie, H., Matsuura, Y., Koike, K., and Miyamura, T. (2002) Interaction of hepatitis C virus core protein with retinoid X receptor alpha modulates its transcriptional activity. *Hepatology* **35**, 937–946
32. Hosui, A., Ohkawa, K., Ishida, H., Sato, A., Nakanishi, F., Ueda, K., Takehara, T., Kasahara, A., Sasaki, Y., Hori, M., and Hayashi, N. (2003) Hepatitis C virus core protein differently regulates the JAK-STAT signaling pathway under interleukin-6 and interferon-gamma stimuli. *J. Biol. Chem.* **278**, 28562–28571
33. Ohkawa, K., Ishida, H., Nakanishi, F., Hosui, A., Ueda, K., Takehara, T., Hori, M., and Hayashi, N. (2004) Hepatitis C virus core functions as a suppressor of cyclin-dependent kinase-activating kinase and impairs cell cycle progression. *J. Biol. Chem.* **279**, 11719–11726
34. Alisi, A., Giambartolomei, S., Cupelli, F., Merlo, P., Fontemaggi, G., Spaziani, A., and Balsano, C. (2003) Physical and functional interaction between HCV core protein and the different p73 isoforms. *Oncogene* **22**, 2573–2580
35. Okabe, H., Satoh, S., Kato, T., Kitahara, O., Yanagawa, R., Yamaoka, Y., Tsunoda, T., Furukawa, Y., and Nakamura, Y. (2001) Genome-wide analysis of gene expression in human hepatocellular carcinomas using cDNA microarray: identification of genes involved in viral carcinogenesis and tumor progression. *Cancer Res.* **61**, 2129–2137
36. Shirota, Y., Kaneko, S., Honda, M., Kawai, H.F., and Kobayashi, K. (2001) Identification of differentially expressed genes in hepatocellular carcinoma with cDNA microarrays. *Hepatology* **33**, 832–840
37. Iizuka, N., Oka, M., Yamada-Okabe, H., Mori, N., Tamesa, T., Okada, T., Takemoto, N., Tangoku, A., Hamada, K., Nakayama, H., Miyamoto, T., Uchimura, S., and Hamamoto, Y. (2002) Comparison of gene expression profiles between hepatitis B virus- and hepatitis C virus-infected hepatocellular carcinoma by oligonucleotide microarray data on the basis of a supervised learning method. *Cancer Res.* **62**, 3939–3944
38. Iizuka, N., Oka, M., Yamada-Okabe, H., Mori, N., Tamesa, T., Okada, T., Takemoto, N., Hashimoto, K., Tangoku, A., Hamada, K., Nakayama, H., Miyamoto, T., Uchimura, S., and Hamamoto, Y. (2003) Differential gene expression in distinct virologic types of hepatocellular carcinoma: association with liver cirrhosis. *Oncogene* **22**, 3007–3014
39. Smith, M.W., Yue, Z.N., Geiss, G.K., Sadovnikova, N.Y., Carter, V.S., Boix, L., Lazaro, C.A., Rosenberg, G.B., Bumgarner, R.E., Fausto, N., Bruix, J., and Katze, M.G. (2003) Identification of novel tumor markers in hepatitis C virus-associated hepatocellular carcinoma. *Cancer Res.* **63**, 859–864
40. Smith, M.W., Yue, Z.N., Korth, M.J., Do, H.A., Boix, L., Fausto, N., Bruix, J., Carithers, R.L., Jr., and Katze, M.G. (2003) Hepatitis C virus and liver disease: global transcriptional profiling and identification of potential markers. *Hepatology* **38**, 1458–1467
41. Takashima, M., Kuramitsu, Y., Yokoyama, Y., Iizuka, N., Toda, T., Sakaida, I., Okita, K., Oka, M., and Nakamura, K. (2003) Proteomic profiling of heat shock protein 70 family members as biomarkers for hepatitis C virus-related hepatocellular carcinoma. *Proteomics* **3**, 2487–2493

42. Yokoyama, Y., Kuramitsu, Y., Takashima, M., Iizuka, N., Toda, T., Terai, S., Sakaida, I., Oka, M., Nakamura, K., and Okita, K. (2004) Proteomic profiling of proteins decreased in hepatocellular carcinoma from patients infected with hepatitis C virus. *Proteomics* **4**, 2111–2116
43. Moradpour, D., Englert, C., Wakita, T., and Wands, J.R. (1996) Characterization of cell lines allowing tightly regulated expression of hepatitis C virus core protein. *Virology* **222**, 51–63
44. Hope, R.G. and McLauchlan, J. (2000) Sequence motifs required for lipid droplet association and protein stability are unique to the hepatitis C virus core protein. *J. Gen. Virol.* **81**, 1913–1925
45. Hope, R.G., Murphy, D.J., and McLauchlan, J. (2002) The domains required to direct core proteins of hepatitis C virus and GB virus-B to lipid droplets share common features with plant oleosin proteins. *J. Biol. Chem.* **277**, 4261–4270
46. Shi, S.T., Polyak, S.J., Tu, H., Taylor, D.R., Gretch, D.R., and Lai, M.M. (2002) Hepatitis C virus NS5A colocalizes with the core protein on lipid droplets and interacts with apolipoproteins. *Virology* **292**, 198–210
47. Harada, T., Kim, D.W., Sagawa, K., Suzuki, T., Takahashi, K., Saito, I., Matsuura, Y., and Miyamura, T. (1995) Characterization of an established human hepatoma cell line constitutively expressing non-structural proteins of hepatitis C virus by transfection of viral cDNA. *J. Gen. Virol.* **76**, 1215–1221
48. Balch, W.E. and Rothman, J.E. (1985) Characterization of protein transport between successive compartments of the Golgi apparatus: asymmetric properties of donor and acceptor activities in a cell-free system. *Arch. Biochem. Biophys.* **240**, 413–425
49. Yanagida, M., Miura, Y., Yagasaki, K., Taoka, M., Isobe, T., and Takahashi, N. (2000) Matrix assisted laser desorption/ionization-time of flight-mass spectrometry analysis of proteins detected by anti-phosphotyrosine antibody on two-dimensional-gels of fibrolast cell lysates after tumor necrosis factor-alpha stimulation. *Electrophoresis* **21**, 1890–1898
50. Yanagida, M., Shimamoto, A., Nishikawa, K., Furuichi, Y., Isobe, T., and Takahashi, N. (2001) Isolation and proteomic characterization of the major proteins of the nucleolin-binding ribonucleoprotein complexes. *Proteomics* **1**, 1390–1404
51. Bligh, E.G. and Dyer, W.J. (1959) A rapid method of total lipid extraction and purification. *Can. J. Med. Sci.* **37**, 911–917
52. Natsume, T., Yamauchi, Y., Nakayama, H., Shinkawa, T., Yanagida, M., Takahashi, N., and Isobe, T. (2002) A direct nanoflow liquid chromatography-tandem mass spectrometry system for interaction proteomics. *Anal. Chem.* **74**, 4725–4733
53. Yanagida, M., Hayano, T., Yamauchi, Y., Shinkawa, T., Natsume, T., Isobe, T., and Takahashi, N. (2004) Human fibrillarin forms a sub-complex with splicing factor 2-associated p32, protein arginine methyltransferases, and tubulins alpha 3 and beta 1 that is independent of its association with preribosomal ribonucleoprotein complexes. *J. Biol. Chem.* **279**, 1607–1614
54. Heid, H.W., Moll, R., Schwetlick, I., Rackwitz, H.R., and Keenan, T.W. (1998) Adipophilin is a specific marker of lipid accumulation in diverse cell types and diseases. *Cell Tissue Res.* **294**, 309–321
55. Londos, C., Brasaemle, D.L., Schultz, C.J., Segrest, J.P., and Kimmel, A.R. (1999) Perilipins, ADRP, and other proteins that associate with intracellular neutral lipid droplets in animal cells. *Semin. Cell Dev. Biol.* **10**, 51–58
56. Wolins, N.E., Rubin, B. and Brasaemle, D.L. (2001) TIP47 associates with lipid droplets. *J. Biol. Chem.* **276**, 5101–5108
57. Miura, S., Gan, J.W., Brzostowski, J., Parisi, M.J., Schultz, C.J., Londos, C., Oliver, B., and Kimmel, A.R. (2002) Functional conservation for lipid storage droplet association among Perilipin, ADRP, and TIP47 (PAT)-related proteins in mammals, Drosophila, and Dictyostelium. *J. Biol. Chem.* **277**, 32253–32257
58. Liu, P., Ying, Y., Zhao, Y., Mundy, D.I., Zhu, M., and Anderson, R.G. (2004) Chinese hamster ovary K2 cell lipid droplets appear to be metabolic organelles involved in membrane traffic. *J. Biol. Chem.* **279**, 3787–3792
59. Fujimoto, Y., Itabe, H., Sakai, J., Makita, M., Noda, J., Mori, M., Higashi, Y., Kojima, S., and Takano, T. (2004) Identification of major proteins in the lipid droplet-enriched fraction isolated from the human hepatocyte cell line HuH7. *Biochim. Biophys. Acta* **1644**, 47–59
60. Brasaemle, D.L., Dolios, G., Shapiro, L., and Wang, R. (2004) Proteomic analysis of proteins associated with lipid droplets of basal and lipolytically stimulated 3T3-L1 adipocytes. *J. Biol. Chem.* **279**, 46835–46842
61. Lu, X., Gruia-Gray, J., Copeland, N.G., Gilbert, D.J., Jenkins, N.A., Londos, C., and Kimmel, A.R. (2001) The murine perilipin gene: the lipid droplet-associated perilipins derive from tissue-specific, mRNA splice variants and define a gene family of ancient origin. *Mamm. Genome* **12**, 741–749
62. Greenberg, A.S., Egan, J.J., Wek, S.A., Moos, M.C., Jr., Londos, C., and Kimmel, A.R. (1993) Isolation of cDNAs for perilipins A and B: sequence and expression of lipid droplet-associated proteins of adipocytes. *Proc. Natl. Acad. Sci. USA* **90**, 12035–12039
63. Diaz, E. and Pfeffer, S.R. (1998) TIP47: a cargo selection device for mannose 6-phosphate receptor trafficking. *Cell* **93**, 433–443
64. Brasaemle, D.L., Barber, T., Wolins, N.E., Serrero, G., Blanchette-Mackie, E.J., and Londos, C. (1997) Adipose differentiation-related protein is an ubiquitously expressed lipid storage droplet-associated protein. *J. Lipid Res.* **38**, 2249–2263
65. Carroll, K.S., Hanna, J., Simon, I., Krise, J., Barbero, P., and Pfeffer, S.R. (2001) Role of Rab9 GTPase in facilitating receptor recruitment by TIP47. *Science* **292**, 1373–1376
66. Pfeffer, S.R. (2001) Rab GTPases: specifying and deciphering organelle identity and function. *Trends Cell Biol.* **11**, 487–491
67. Blot, G., Janvier, K., Le Panse, S., Benarous, R., and Berlioz-Torrent, C. (2003) Targeting of the human immunodeficiency virus type 1 envelope to the trans-Golgi network through binding to TIP47 is required for env incorporation into virions and infectivity. *J. Virol.* **77**, 6931–6945
68. Serfaty, L., Andreani, T., Giral, P., Carbonell, N., Chazouilleres, O., and Poupon, R. (2001) Hepatitis C virus induced hypobetalipoproteinemia: a possible mechanism for steatosis in chronic hepatitis C. *J. Hepatol.* **34**, 428–434
69. Perlemuter, G., Sabile, A., Letteron, P., Vona, G., Topilco, A., Chretien, Y., Koike, K., Pessayre, D., Chapman, J., Barba, G., and Brechot, C. (2002) Hepatitis C virus core protein inhibits microsomal triglyceride transfer protein activity and very low density lipoprotein secretion: a model of viral-related steatosis. *FASEB J.* **16**, 185–194
70. Owsianka, A.M. and Patel, A.H. (1999) Hepatitis C virus core protein interacts with a human DEAD box protein DDX3. *Virology* **257**, 330–340
71. Mamiya, N. and Worman, H.J. (1999) Hepatitis C virus core protein binds to a DEAD box RNA helicase. *J. Biol. Chem.* **274**, 15751–15756
72. Gururajan, R. and Weeks, D.L. (1997) An3 protein encoded by a localized maternal mRNA in Xenopus laevis is an ATPase with substrate-specific RNA helicase activity. *Biochim. Biophys. Acta* **1350**, 169–182
73. Chen, H.C., Lin, W.C., Tsay, Y.G., Lee, S.C., and Chang, C.J. (2002) An RNA helicase, DDX1, interacting with poly(A) RNA and heterogeneous nuclear ribonucleoprotein K. *J. Biol. Chem.* **277**, 40403–40409
74. Dvorak, A.M., Morgan, E.S., and Weller, P.F. (2003) RNA is closely associated with human mast cell lipid bodies. *Histol. Histopathol.* **18**, 943–968
75. Godbout, R., Packer, M., and Bie, W. (1998) Overexpression of a DEAD box protein (DDX1) in neuroblastoma and retinoblastoma cell lines. *J. Biol. Chem.* **273**, 21161–21168

76. Huang, J.S., Chao, C.C., Su, T.L., Yeh, S.H., Chen, D.S., Chen, C.T., Chen, P.J., and Jou, Y.S. (2004) Diverse cellular transformation capability of overexpressed genes in human hepatocellular carcinoma. *Biochem. Biophys. Res. Commun.* **315**, 950–958
77. Liu, M., Liu, Y., Cheng, J., Zhang, S.L., Wang, L., Shao, Q., Zhang, J., and Yang, Q. (2004) Transactivating effect of hepatitis C virus core protein: a suppression subtractive hybridization study. *World J. Gastroenterol.* **10**, 1746–1749
78. Ohkawa, K., Ishida, H., Nakanishi, F., Hosui, A., Sato, A., Ueda, K., Takehara, T., Kasahara, A., Sasaki, Y., Hori, M., and Hayashi, N. (2003) Changes in gene expression profile by HCV core protein in cultured liver cells: analysis by DNA array assay. *Hepatol. Res.* **25**, 396–408
79. Sacco, R., Tsutsumi, T., Suzuki, R., Otsuka, M., Aizaki, H., Sakamoto, S., Matsuda, M., Seki, N., Matsuura, Y., Miyamura, T., and Suzuki, T. (2003) Antiapoptotic regulation by hepatitis C virus core protein through up-regulation of inhibitor of caspase-activated DNase. *Virology* **317**, 24–35

Journal of Bioinformatics and Computational Biology
Vol. 4, No. 2 (2006) 469–482

Imperial College Press
www.icpress.co.uk

COMPARATIVE GENOMIC ANALYSIS OF TRANSCRIPTION REGULATION ELEMENTS INVOLVED IN HUMAN MAP KINASE G-PROTEIN COUPLING PATHWAY

NATALIA POLOULIAKH

Computational Biology Research Center
National Institute of Advanced Industrial Science and Technology
Aomi 2-42, Koto-ku, Tokyo, 153 – 0061, Japan
nata.polouliakh@aist.go.jp

TOHRU NATSUME

Japan Biological Information Research Center
National Institute of Advanced Industrial Science and Technology
Aomi 2-42, Koto-ku, Tokyo, 153 – 0061, Japan
natsume@jbirc.aist.go.jp

HAJIME HARADA*, WATARU FUJIBUCHI† and PAUL HORTON‡

Computational Biology Research Center
National Institute of Advanced Industrial Science and Technology
Aomi 2-42, Koto-ku, Tokyo, 153 – 0061, Japan
**harada-hajime@aist.go.jp*
†*fujibuchi-wataru@aist.go.jp*
‡*horton-p@aist.go.jp*

Received 30 September 2005
Revised 22 November 2005
Accepted 8 December 2005

The identification of *cis*-elements (motifs) in the regulatory regions of higher eukaryotes is an important and challenging problem in computational biology. Eukaryotic transcriptional regulatory mechanisms pose several difficulties for promoter analysis: including a high variance in the motif locations, frequently large divergence from motif consensus patterns, and a large amount of repetitive elements (confusing to many motif finding procedures). One promising approach to this difficult problem involves cross-species comparison. In this work we analyzed the full-length regulatory regions of genes involved in the G-protein coupling MAP kinase pathway and compared the results with ribosomal genes using human, mouse and rat genomic data. We found 19 high likely transcription factors (TFs) candidates for MAPK and 12 TFs for the ribosomal dataset. In the case of the MAPK dataset, regulatory regions of genes functionally grouped as receptors and MAP-core genes were found mostly highly conserved across the three species.

Keywords: MAPK; promoter analysis; *cis*-element.

1. Introduction

1.1. *History of MAPK pathway study*

Mitogen-activated protein kinases (MAPKs) are important signal transduction enzymes, unique to eukaryotes, connecting cell-surface receptors to critical regulatory targets within the cell. MAPKs are involved in cell survival and adaptation. MAPKs activity is regulated through three-tiered cascades composed of a MAPK, a MAPK kinase (MAPKK) and a MAPKK kinase (MAPKKK); in mammals this cascade is implemented by ERK, MEK and RAF as depicted in Fig. 1. MEK (MAPKK) is itself activated by phosphorylation catalyzed by the first kinase RAF (MAPKKK), which is activated by the small GTP-binding G protein Ras in mammalian pathways.[1] In this paper we present a transcriptional analysis of some genes in this pathway in the context of protein-protein interaction (PPI) data (Natsume *et al.*, in preparation).

The MAPK pathway used in this study is activated by signaling through PTK (protein tyrosine kinase) receptor protein, which is a type I transmembrane proteins with a cytoplasmic domain, that has intrinsic catalytic activity that is activated upon ligand binding.[2] Ligand-induced dimerization juxtaposes the two catalytic domains of receptors allowing mutual transphosphorylation of residues in the activation loop of the catalytic domain, leading to enzymatic activation, and autophosphorylation of several tyrosines, inducing the GTP-binding conformational state of Ras, which activates the three above mentioned kinases: RAF (MAPKKK), MEK

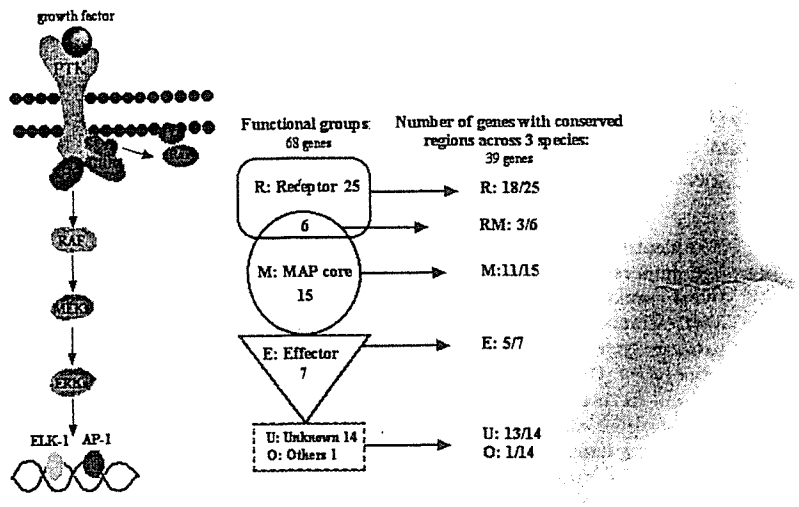

Fig. 1. A schematic view of the receptor PTK pathway and functional groups with the respective number of genes. The number of genes in which we obtained three-species orthologous promoter alignment is pointed to by arrows for each functional group. For example, in the group of "Receptor – MAP core genes" (RM), 3 out of 6 genes alignment was obtained across human, mouse and rat.